NASA TECHNICAL MEMORANDUM

NASA TM X-2376

NASA TM X-2376

ANALYSIS OF HEAT-TRANSFER TESTS OF AN IMPINGEMENT-CONVECTION- AND FILM-COOLED VANE IN A CASCADE

by Herbert J. Gladden, Daniel J. Gauntner, and John N. B. Livingood

Lewis Research Center
Cleveland, Ohio 44135

NATIONAL AERONAUTICS AND SPACE ADMINISTRATION • WASHINGTON, D. C. • DECEMBER 1971

1. Report No.	2. Government Accession No.	3. Recipient's Catalog No.
NASA TM X-2376		

4. Title and Subtitle	5. Report Date
ANALYSIS OF HEAT-TRANSFER TESTS OF AN IMPINGEMENT-CONVECTION- AND FILM-COOLED VANE IN A CASCADE	December 1971
	6. Performing Organization Code
7. Author(s) Herbert J. Gladden, Daniel J. Gauntner, and John N. B. Livingood	8. Performing Organization Report No. E-6230
	10. Work Unit No. 764-74
9. Performing Organization Name and Address Lewis Research Center National Aeronautics and Space Administration Cleveland, Ohio 44135	11. Contract or Grant No.
	13. Type of Report and Period Covered Technical Memorandum
12. Sponsoring Agency Name and Address National Aeronautics and Space Administration Washington, D.C. 20546	14. Sponsoring Agency Code

15. Supplementary Notes

16. Abstract

Experimental flow and heat-transfer data obtained for an air-cooled turbine vane tested in a static cascade at gas temperatures and pressures to 1644 K (2500° F) and 31 N/cm^2 (45 psia), respectively, are presented. Average and local vane temperatures are correlated in several ways. Calculated and measured coolant flows and vane temperatures are compared. Potential allowable increases in gas temperature are also discussed.

17. Key Words (Suggested by Author(s))	18. Distribution Statement
Turbine cooling; Heat transfer; Impingement cooling; Film cooling; Convection cooling; Pin fins; Airfoil temperature correlations; Analytical temperature comparison	Unclassified - unlimited

19. Security Classif. (of this report)	20. Security Classif. (of this page)	21. No. of Pages	22. Price*
Unclassified	Unclassified	46	$3.00

*For sale by the National Technical Information Service, Springfield, Virginia 22151

ANALYSIS OF HEAT-TRANSFER TESTS OF AN IMPINGEMENT-CONVECTION- AND FILM-COOLED VANE IN A CASCADE

by Herbert J. Gladden, Daniel J. Gauntner, and John N. B. Livingood

Lewis Research Center

SUMMARY

An experimental investigation of the heat-transfer and flow characteristics of an air-cooled turbine vane operated in a cascade to a gas temperature and pressure of 1644 K (2500° F) and 31 N/cm^2 (45 psia), respectively, is discussed. The experimental data were used to develop heat-transfer correlations for average vane midspan conditions and for selected local midspan positions. Lack of measured cooling-air temperatures, except at the coolant inlet, affected the correlations. The correlation which gives a temperature difference ratio as a function of the ratio of coolant flow to gas flow is the one recommended. This correlation is the simplest to apply, serves as a basis for comparison of vanes of different cooling configurations, and is applicable for design calculations.

Calculated flow rates and vane wall temperatures are compared with experimental values. The calculated flow results were achieved by the use of some empirical flow data obtained in separate flow tests for the particular vane considered. Favorable comparisons were achieved.

As a measure of the vane cooling efficiency, the experimental results showed that for a turbine inlet temperature of 1644 K (2500° F), a coolant inlet temperature of 589 K (600° F), and a ratio of coolant flow to gas flow of 0.035, the average vane wall temperature was 1159 K (1626° F). From these values, it can be noted that the vane was cooled effectively.

INTRODUCTION

An experimental investigation was made to determine the heat-transfer characteristics of an air-cooled turbine vane, to evaluate heat-transfer correlation methods, and to compare analytical and measured vane temperatures and coolant flows.

Materials currently in use for the fabrication of turbine vanes and blades are being pushed to the limit of their structural capabilities. High-performance engines of the future will operate at increased turbine inlet temperatures. To design these vanes and blades, it is necessary to accurately predict the wall temperatures. Ideally, wall temperatures should be predicted analytically. Attempts at developing adequate analytical prediction methods are in progress; however, until such methods become perfected, empirical correlations like those developed herein will be required for estimating wall temperatures. Successful correlation of the data taken over a limited range of variables should permit the estimation of wall temperatures for any set of operating conditions and the elimination of a vast amount of testing. Also, different internal cooling configurations may be compared by their cooling effectiveness.

Methods for calculating the spanwise temperature distribution in an air-cooled turbine vane or blade are presented in reference 1. One of the equations in reference 1 was modified and used to correlate experimental data for the leading-edge region of a turbine blade in reference 2. Reference 3 presents a method for comparing the cooling effectiveness of vanes and blades with different cooling configurations. Further modifications of the method of reference 1 are made herein in order to correlate experimental vane temperatures over the complete vane surface.

The heat-transfer tests reported herein were made in a cascade facility (described in ref. 4) which was capable of operation at gas temperatures to 1644 K (2500° F) and gas pressures to 103.4 N/cm^2 (150 psia). Tests were conducted for gas temperatures from 700 to 1644 K (800° to 2500° F), gas pressures from 12.4 to 31.1 N/cm^2 (18 to 45 psia), coolant temperatures from 291 to 922 K (65° to 1200° F), and ratios of coolant flow to gas flow from 0.02 to 0.15.

The results referred to herein as analytical were obtained by adapting a computer program to a Lewis computer and incorporating some flow data determined experimentally in a separate flow facility. This adaptation was done by John E. Rohde.

APPARATUS

Facility Description

The cascade facility was designed for continuous operation at 1644 K (2500° F) and 103.4 N/cm^2 (150 psia). A schematic cross-sectional view of the cascade is shown in figure 1(a). The facility consisted of five components: an inlet section, a burner section, a circular-to-annular transition section, the test section, and an exit section. The transition, test, and exit sections were water cooled to achieve structural durability during high-temperature operation. A more detailed description is contained in reference 4.

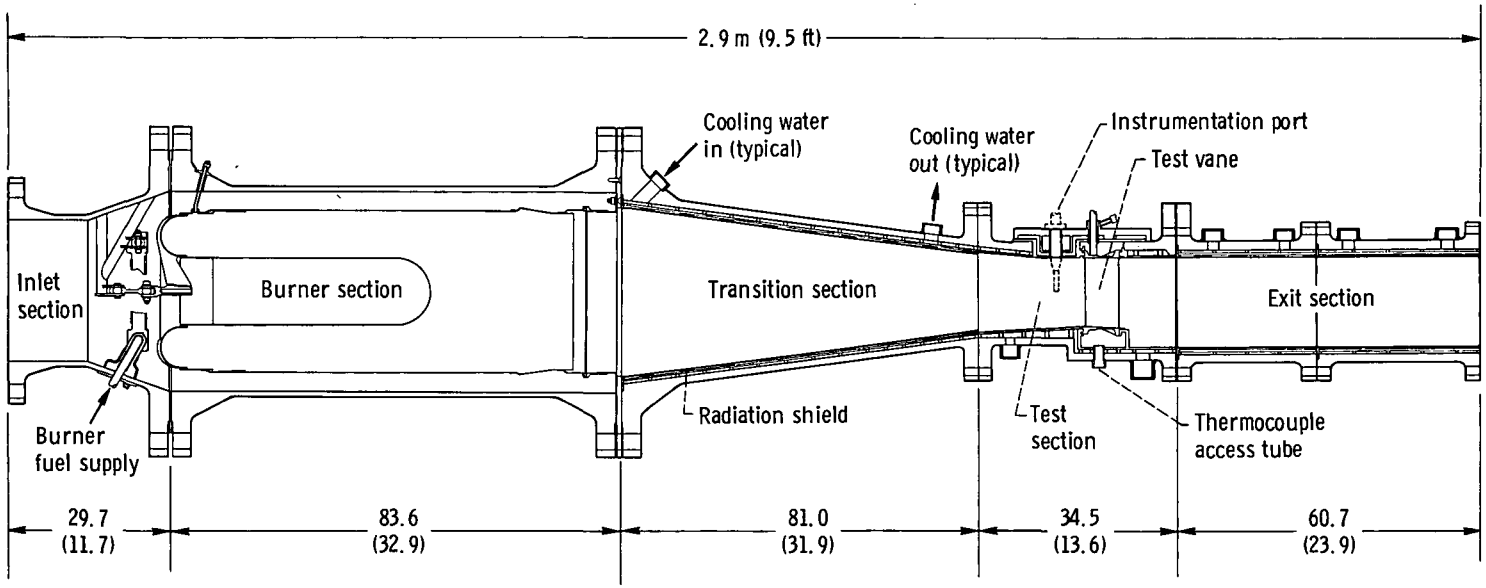

(a) Schematic cross-sectional view of main components. (Dimensions are in cm (in.), unless noted.)

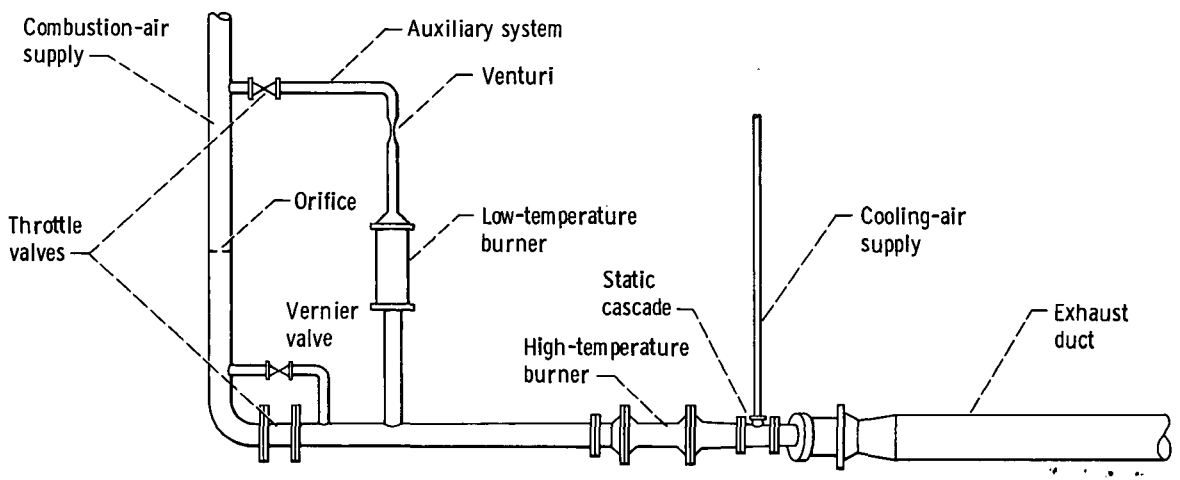

(b) Schematic showing low-temperature burner.

Figure 1. - Schematic view of cascade facility.

For low-temperature tests the burner section was removed and replaced by a spool piece. Combustion air was then supplied to the test section by the auxiliary system shown in figure 1(b). The burner in the auxiliary system was capable of supplying combustion gas at temperatures to 922 K (1200° F). The gas temperature profile provided to the vane row by the low-temperature burner had a maximum- to average-temperature ratio of 1.011 or less. The high-temperature burner had a temperature ratio of 1.025 or less at 1644 K (2500° F) and 1.051 at 922 K (1200° F).

The test section (fig. 1(a)) represented an annular sector of a vane row and contained four vanes and five flow channels. A top view of the test section with the access cover removed is shown in figure 2. A vane pack assembly is shown in place. Extending above the vane pack are the cooling-air supply tubes for each vane. The central two vanes were connected to a common air supply plenum, while the outer vanes were connected to separate air supply systems. Figure 3 is a schematic top view of the test section. The central vanes could also be supplied by a vitiated air heater capable of operation at temperatures to 922 K (1200° F). The four vane positions and five flow channels are numbered from left to right. The central vanes (positions 2 and 3) are referred to as test vanes, and the outer vanes (positions 1 and 4) are referred to as slave vanes.

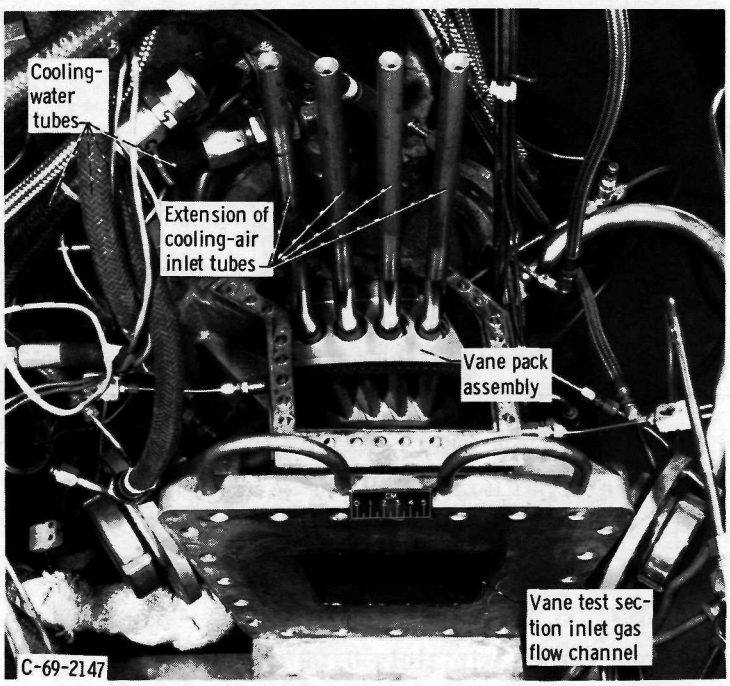

Figure 2. - Top view of cascade test section with access cover removed.

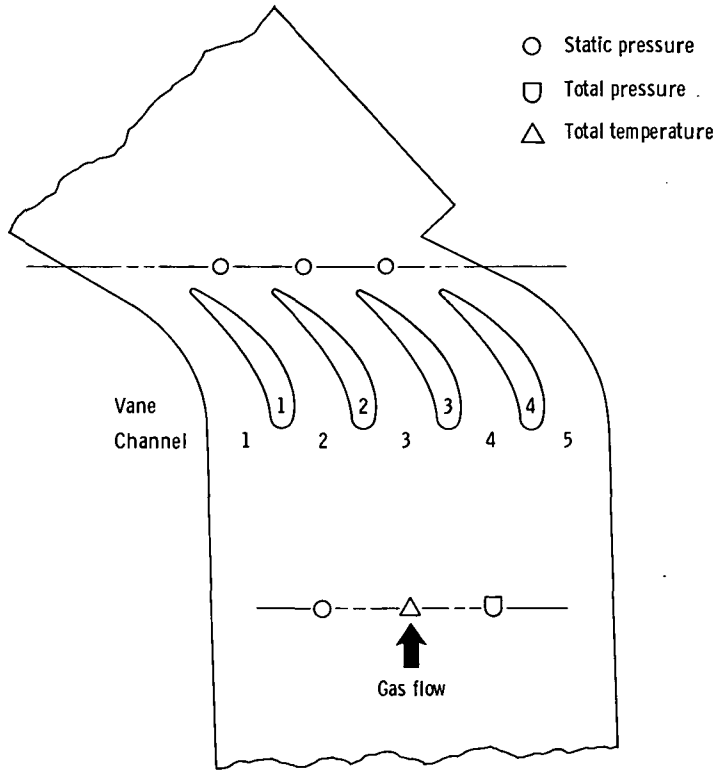

Figure 3. - Schematic top view of test section (1644 K (2500° F) cascade).

Vane Description

The vane cooling configuration tested during this investigation is shown schematically in figure 4. (Symbols are defined in appendix A.) The vane span was 9.78 centimeters (3.85 in.) and the midspan chord length was 6.28 centimeters (2.47 in.). Cooling air entered the vane from the supply tube located at the tip or outer diameter of the vane. From a tip plenum chamber the airflow divided in two parts, with approximately 25 percent entering the leading-edge impingement tube while the remainder entered the midchord supply tube. The airflow which entered the leading edge flowed through 16 slots and impinged on the internal surface of the leading edge. The slots were 0.47 centimeter (0.185 in.) long and 0.02 to 0.038 centimeter (0.008 to 0.015 in.) wide. The leading-edge inside surface area was increased by chordwise fins which were 0.102 to 0.127 centimeter (0.04 to 0.05 in.) deep and 0.038 to 0.051 centimeter (0.015 to 0.020 in.) wide. The fin pitch was approximately 0.09 centimeter (0.035 in.). The airflow then passed around the impingement tube in a chordwise direction and into an exit collector passage. This air then flowed to the hub or inner diameter platform and exited into a chamber which, in turn, vented into the cascade exit section. The airflow which entered the midchord supply tube impinged on the internal surfaces of the vane suction

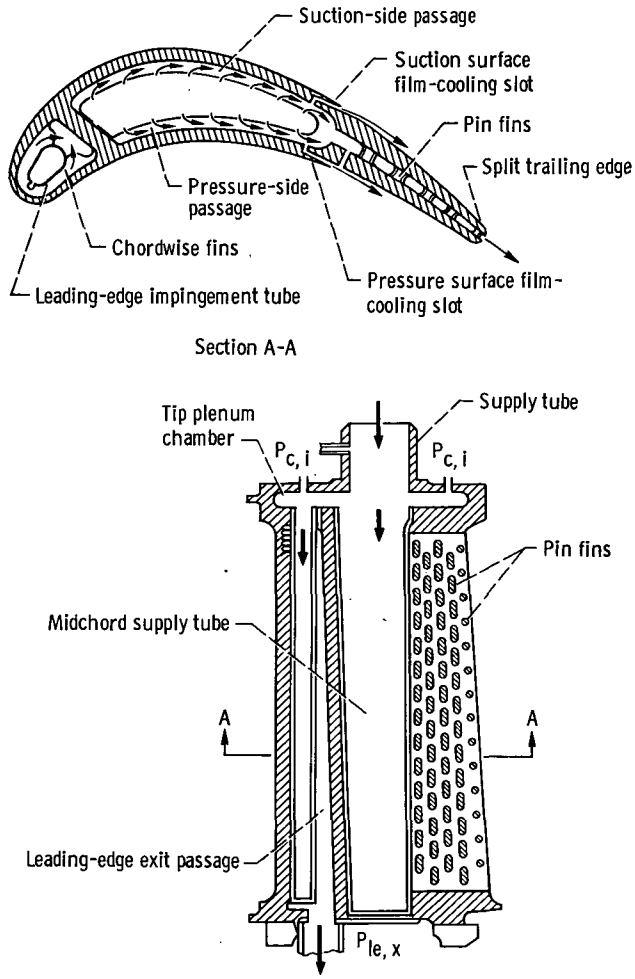

Figure 4. - Vane internal flow configuration.

and pressure sides by flowing through an array of 0.038-centimeter (0.015-in.) diameter holes. There were 481 and 334 holes, respectively, on the suction and pressure sides. This flow then exited from the vane through film-cooling slots on the suction and pressure surfaces, and through a split trailing edge containing pin fins. The pressure surface film-cooling slot was a continuous slot 9.27 centimeters (3.65 in.) by 0.064 centimeter (0.025 in.) which was fed by 16 metering slots 0.25 centimeter (0.10 in.) by 0.053 centimeter (0.021 in.). The suction surface contained eight slots 1.11 centimeters (0.438 in.) by 0.051 centimeter (0.020 in.), which were fed by 16 metering slots 0.19 centimeter (0.075 in.) by 0.051 centimeter (0.020 in.). There were four rows of oblong pin fins in the trailing edge which were 0.38 centimeter (0.15 in.) by 0.25 centimeter (0.10 in.) and varied in height from 0.18 centimeter (0.070 in.) to 0.094 centimeter (0.037 in.). A single row of round pin fins had a diameter of 0.20 centimeter (0.08 in.) and a height of 0.064 centimeter (0.025 in.), see figure 4.

INSTRUMENTATION

The instrumentation utilized by the cascade can be separated into two categories: the general operational instrumentation and the research instrumentation. The operational instrumentation was used to set data points and to monitor the general condition of the cascade and its supporting systems. Most of this instrumentation was connected to visual readouts in the control room. The research instrumentation was concentrated on or around the test vanes and was designed to provide data for detailed analysis of the cooling performance of the test vanes. Most of these data were recorded by a central data recording system. Reference 4 contains a more detailed description of the cascade instrumentation and data recording system.

Operational Instrumentation

The cascade was equipped with the general instrumentation required to monitor quantities such as combustion gas total inlet temperature and pressure; vane row exit static pressures; fuel flow rate, temperature, and pressure; cooling-water flow rate, temperature, and pressure; and the various cooling-air flow rates, temperatures, and pressures.

Research Instrumentation

The purpose of the research instrumentation was to provide detailed information on the gas stream conditions, the cooling-air flow conditions, and the vane wall temperature distribution. Radially traversing total temperature and total pressure probes were located upstream of the vane row (fig. 3). Briefly, the total temperature distribution was measured in front of channel 3, and the total pressure distribution was measured in front of channel 4. Figure 3 indicates a static pressure measurement in front of channel 2; however, the static pressure was measured only at the hub platform and was assumed to be constant across the gas stream. Static pressures were also measured at the exit midchannel position at both the hub and tip platforms. These pressures were used to establish the midspan exit Mach number.

Each test vane was instrumented with an array of 25 thermocouples and 13 coolant-passage static pressure taps. Figure 5(a) is a schematic layout of the thermocouples and pressure taps. Three spanwise locations (hub, midspan, and tip) were instrumented. The hub and tip sections were located approximately 1.63 centimeters (0.64 in.) from the respective platforms. The midspan of the test vanes contained 13 of the 25 thermocouples and the hub and tip sections contained six thermocouples each. Thermocouple

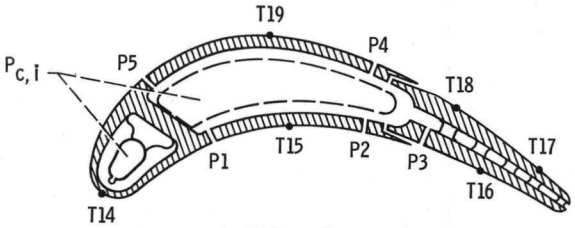

(a-1) Tip section.

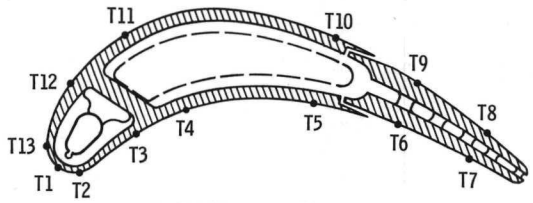

(a-2) Midspan section.

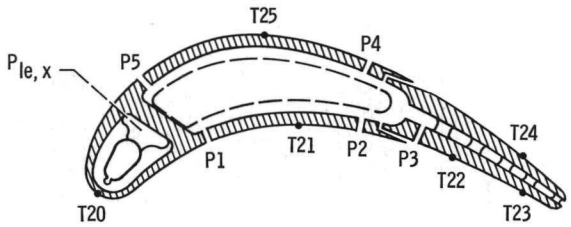

(a-3) Hub section.

(a) Schematic showing location of thermocouples and pressure taps for hub, midspan, and tip sections.

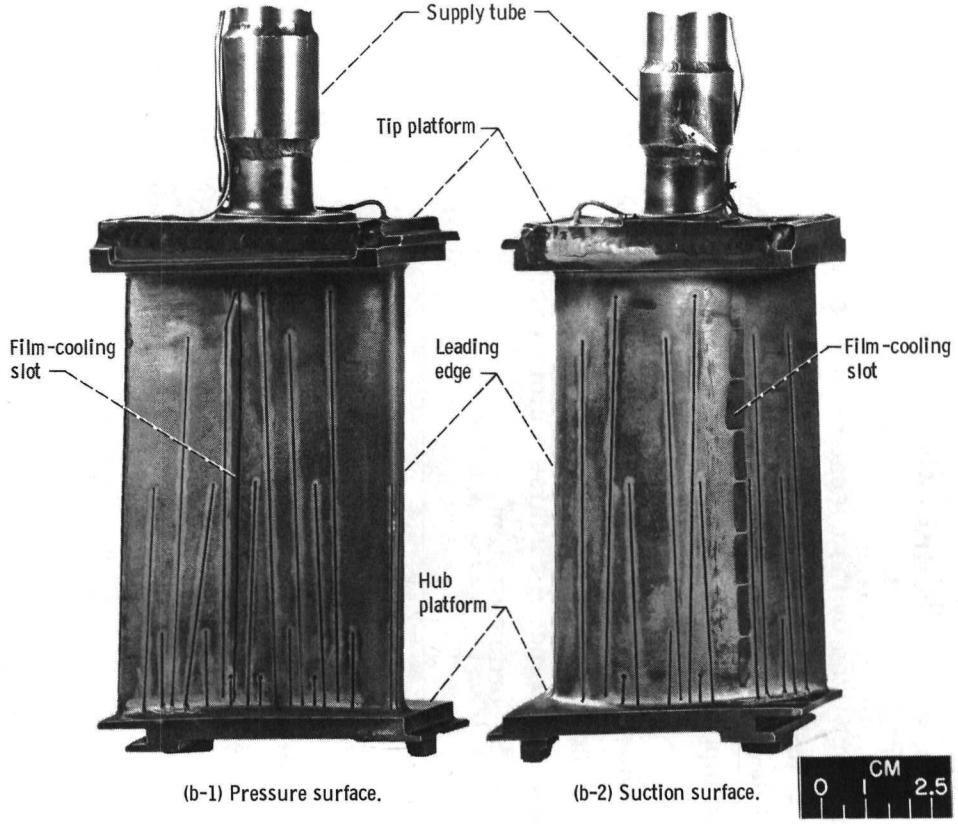

(b-1) Pressure surface.

(b-2) Suction surface.

(b) View of suction and pressure surfaces of test vanes, showing instrumented slots.

Figure 5. - Test vane instrumentation.

TABLE I. - LOCATION OF THERMOCOUPLES SHOWN IN FIGURES 5(a) AND (b)

(a) Tip section. Length of suction surface, L_S = 7.3 cm (2.87 in.); length of pressure surface, L_P = 6.5 cm (2.56 in.)

Suction surface				Pressure surface			
Thermocouple	Surface distance, x		Dimensionless surface distance, x/L_S	Thermocouple	Surface distance, x		Dimensionless surface distance, x/L_P
	cm	in.			cm	in.	
14	0	0	0	15	2.65	1.045	0.408
19	3.0	1.22	.425	16	4.9	1.93	.753
18	5.4	2.125	.74				
17	6.45	2.54	.885				

(b) Midspan section. Length of suction surface, L_S = 7.27 cm (2.86 in.); length of pressure surface, L_P = 6.53 cm (2.57 in.)

1	0	0	0	2	0.394	0.155	0.06
13	.318	.125	.044	3	.97	.38	.148
12	.81	.32	.112	4	2.08	.82	.319
11	2.29	.90	.315	5	3.42	1.345	.524
10	3.91	1.54	.539	6	4.37	1.72	.67
9	5.27	2.075	.727	7	5.69	2.24	.872
8	6.18	2.435	.852				

(c) Hub section. Length of suction surface, L_S = 7.26 cm (2.86 in.); length of pressure surface, L_P = 6.58 cm (2.59 in.)

20	0	0	0	21	2.65	1.045	0.402
25	3.21	1.265	.443	22	4.5	1.77	.683
24	7.2	2.835	.992	23	5.47	2.155	.832

locations are given in table I. There were five pressure taps in each of the hub and tip sections. There were also two pressure taps in the tip plenum: one over the leading-edge impingement tube, and one over the midchord insert. The leading-edge exhaust pressure was also measured (see fig. 4). The coolant-passage pressure taps were arranged such that local flow rates could be calculated from the pressure drop distribution and local calibration data contained in reference 5. Figure 5(b) shows the suction surface of vane 2 and the pressure surface of vane 3.

The construction of the thermocouple assemblies consisted of Chromel-Alumel wire with magnesium oxide insulation in an Inconel-600 sheath. These assemblies were drawn to two sizes, 0.051 and 0.025 centimeter outside diameter (20 and 10 mil), with a closed-end grounded thermocouple junction formed at one end. The five thermocouples

nearest the leading edge were of 0.025 centimeter (10 mil) outside diameter while the remaining thermocouples were of 0.051 centimeter (20 mil) outside diameter.

A detailed description of procedures utilized for thermocouple construction is given in reference 6.

EXPERIMENTAL PROCEDURE

An experimental investigation was made over a sufficiently wide variation in operating conditions so that reliable heat-transfer correlations could be determined. The parameters varied included the combustion gas total temperature and total pressure and also the inlet coolant temperature and flow rate. A base-point design condition for the combustion gas was established as 1644 K (2500° F) at 31 N/cm^2 (45 psia) with a trailing-edge, midspan, midchannel Mach number of 0.85. The design inlet coolant temperature for this combustion gas condition was 922 K (1200° F).

Two additional inlet coolant temperatures were investigated for the design combustion gas condition: 589 K (600° F) and 300 K (80° F).

Variations in the combustion gas conditions were also investigated so that a wide range of gas flow rates could be used in the correlation of the data. Combustion gas total temperatures of 700 K (800° F) and 922 K (1200° F) were run at a total pressure of 12.4 N/cm^2 (18.0 psia). Data were also taken for combustion gas total temperatures of 811 K (1000° F) and 922 K (1200° F) at a total inlet pressure of 24.8 N/cm^2 (36.0 psia). Inlet coolant temperatures of 292 K (65° F) and 456 K (360° F) were run over a range of flow rates for these combustion gas conditions. The various test conditions are summarized in table II. Also contained in table II is a common symbol list used for most of the curves.

The cascade operating procedure was essentially the same for both the high-temperature burner and the low-temperature burner. After burner ignition, the desired combustion gas flow rate and pressure were established by adjusting inlet and exhaust throttle valves while maintaining the desired total temperature by an automatic controller. The combustion gas flow rate was adjusted until the desired exit static- to total-pressure ratio was attained. For control purposes, the hub and tip exit static pressures were averaged and ratioed to the inlet total pressure. (The inlet and exit total pressures were assumed to be equal.) When the desired combustion gas conditions were established, the coolant flow rate was varied in a stepwise fashion at a given coolant inlet temperature. The ratio of coolant flow to combustion gas flow ranged from approximately 0.02 to 0.15.

a

TABLE II. - SUMMARY OF TEST CONDITIONS

Combustion gas conditions				Inlet coolant conditions				Common symbols
Inlet total temperature		Inlet total pressure		Temperature		Coolant-to-gas temperature ratio	Ratio of coolant flow to gas flow, $\dot{w}_c/\dot{w}_g$	
K	^{o}F	N/cm^2	psia	K	^{o}F			
1644	2500	31.1	45	[a]922	1200	0.561	0.06 to 0.13	□
1644	2500	31.1	45	589	600	.358	0.03 to 0.15	□
1644	2500	31.1	45	300	80	.182	0.03 to 0.15	□
811	1000	12.4	18	456	360	.561	0.03 to 0.15	▷
811	1000	↓	↓	292	65	.358	0.02 to 0.15	⌂
700	800			292	65	.416	0.02 to 0.15	◁
922	1200			292	65	.316	0.02 to 0.15	◿
922	1200			456	360	.494	0.03 to 0.15	◺
811	1000	24.8	36	292	65	.358	0.02 to 0.15	▷
922	1200	24.8	36	292	65	.316	0.02 to 0.15	△
922	1200	24.8	36	456	360	.494	0.03 to 0.15	◁

[a]Data at this coolant temperature were of doubtful accuracy and thus were not used to determine the experimental correlation.

ANALYSIS METHODS

The determination of vane (or blade) wall temperatures depends on a knowledge of certain gas-side factors. The pressure distribution around the vane (or blade) is required in order to determine both the coolant flow distribution through the internal coolant passages and the velocity distribution around the external profile. The pressure and velocity distributions are needed in order to evaluate the convection gas-to-metal heat-transfer coefficient. The effective gas temperature distribution is also required and is used in conjunction with the convection gas-to-wall heat-transfer coefficient distribution to evaluate local values of the wall temperature. For parts of the vane (or blade) that are film cooled, the film-cooling effectiveness is also required in order to evaluate the adiabatic wall temperature and, when used with the convection gas-to-wall heat-transfer coefficient, to determine the wall temperature.

Pressure Distribution

The pressure distribution around the vane may be obtained either experimentally or analytically. Since an experimental pressure distribution is usually not available, a calculated pressure distribution is required. The pressure distribution is obtained from

a calculated velocity distribution. Two methods for calculating the velocity distribution around an airfoil are given in references 7 and 8. The velocity distribution calculated by the method of reference 7 was used to obtain an analytical pressure distribution around the vane; this distribution was favorably compared in reference 9 to an experimental distribution obtained for the same airfoil shape in the cascade facility for both design and off-design Mach numbers.

Convection Gas-to-Wall Heat-Transfer Coefficients

For the vane leading-edge region, the Nusselt correlation for flow over a cylinder was used. It is (ref. 10, p. 373)

$$Nu_g = 1.14\,Re^{0.5}Pr^{0.4}\left(1 - \left|\frac{\theta}{90}\right|^3\right) \tag{1}$$

where θ, the angle measured from the stagnation point, may vary from -80° to 80°.

For the other parts of the vane, the turbulent flow flat-plate correlation was used. It is (ref. 11, p. 198)

$$Nu_g = 0.0296\,Re^{0.8}Pr^{1/3} \tag{2}$$

Equations (1) and (2) were evaluated at the reference temperature (ref. 12)

$$T_{ref} = 0.28\,T_{st} + 0.5\,T_w + 0.22\,T_{ge} \tag{3}$$

Effective Gas Temperature

The local effective gas temperature is obtained from the equation

$$T_{ge} = T'' - (1 - \Lambda)\frac{W_y^2}{2gJC_p} \tag{4}$$

In this equation, T'' is the relative total temperature, W_y is the relative local velocity, and Λ is the recovery factor. For turbulent flow, $\Lambda = Pr^{1/3}$; for laminar flow, $\Lambda = Pr^{1/2}$.

Film-Cooling Effectiveness

The trailing-edge region of the vane considered herein was film cooled. Hence, the film-cooling effectiveness for the suction surface and pressure surface trailing-edge region had to be evaluated. This was accomplished by use of the correlation, taken from reference 13,

$$\eta_f = \frac{1}{1 + c_m \frac{x}{Ms}} \tag{5}$$

where c_m is a mixing coefficient indicating the level of turbulence. For use herein, a value of $c_m = 0.01$ was used (ref. 14).

The value of η_f obtained from the selected equation was used to determine the adiabatic wall temperature from the equation

$$\eta_f = \frac{T_{ge} - T_{aw}}{T_{ge} - T_{c,s}} \tag{6}$$

This adiabatic wall temperature was used in place of the effective gas temperature for determining the heat flux to a film-cooled surface.

Experimental Vane Wall Temperature Correlations

Since purely analytical methods for predicting vane wall temperatures have not yet been perfected, it was necessary to use empirical correlations for estimating vane temperatures. The following paragraphs describe several correlations.

Correlation equations. - When a surface is convection cooled or convection heated, it is possible to correlate experimental data obtained for different gas flow rates, coolant flow rates, gas temperatures, and coolant temperatures. Several correlations are derived in appendix B. One such correlation is given by equation (B12) for a convection-cooled wall.

$$Y = K\left(\frac{\dot{w}}{\mu}\right)_g^n \left(\frac{\mu}{\dot{w}}\right)_c^m \tag{B12}$$

where

$$Y = \frac{1 - \varphi}{\varphi} \frac{Pr_c^{1/3} k_c}{Pr_g^{1/3} k_g} \tag{B11}$$

$$\varphi = \frac{T_{ge} - T_w}{T_{ge} - T_c} \tag{B3}$$

and m and n are exponents which are discussed later and K is the slope of the line correlating Y and

$$\left(\frac{\dot{w}}{\mu}\right)_g^n \left(\frac{\mu}{\dot{w}}\right)_c^m$$

Some surfaces are cooled by a combination of convection and film cooling. The trailing-edge region of the vane under consideration and shown in figure 4 illustrates this combined cooling. Film-cooling slots appear on both the suction and pressure surfaces of the vane in the trailing-edge region, and the split trailing edge contains five rows of pin fins for added convection cooling.

A method for correlating data for surfaces cooled by a combination of convection cooling and film cooling is derived in appendix B. The correlation is given by equation (B10)

$$\frac{Y}{\left(\frac{\dot{w}}{\mu}\right)_g^n \left(\frac{\mu}{\dot{w}}\right)_c^m} = K\left[1 - \frac{\eta_f}{\varphi}\left(\frac{T_{ge} - T_{c,s}}{T_{ge} - T_c}\right)\right] \tag{B10}$$

When η_f is zero (no film cooling), the correlation equation (eq. (B10)) reduces to equation (B12) (for convection cooling only).

Correlation of data was attempted using both equations (B10) and (B12).

Simplification of correlations. - The correlation equations derived in appendix B and discussed in the preceding section are quite complicated to apply. Under certain conditions, for the sake of ease in application, it is advisable to simplify these correla-

tions. For example, if the cooling-air and gas properties are assumed to be constant over the range of temperatures considered, equation (B12) reduces to

$$\frac{1 - \varphi}{\varphi} = K_3 \frac{\dot{w}_g^n}{\dot{w}_c^m} \tag{7}$$

Data obtained for an air-cooled turbine blade containing tubes as coolant passages were correlated by plotting $\varphi/\dot{w}_c^m$ against $\dot{w}_g$ in reference 15. This correlation, like that suggested by equation (7) involved powers of the coolant flow and gas flow rates.

A further simplification is possible by assuming $m = n$ in equation (7) and plotting φ against $\dot{w}_c/\dot{w}_g$. A least-squares fit of $(1 - \varphi)/\varphi$ against $\dot{w}_g/\dot{w}_c$ gives the constants required in the correlation equation for φ.

$$\varphi = \frac{1}{1 + K_3\left(\frac{\dot{w}_g}{\dot{w}_c}\right)^n} \tag{8}$$

This procedure was followed to determine the φ correlation equations.

A correlation useful in comparing the cooling effectivenesses of vanes and blades with different internal cooling configurations was derived in reference 3. It is

$$\varphi = \frac{1}{\frac{F}{\eta_t} + 1} \tag{9}$$

where φ is defined by equation (B3). The thermal effectiveness η_t given by

$$\eta_t = \frac{T_{c,o} - T_{c,i}}{\overline{T}_w - T_{c,i}} \tag{10}$$

and F is defined as

$$F = \frac{h_g S_g}{\dot{w}_c C_{p,c}} \tag{11}$$

An attempt to determine the cooling effectiveness of the vane discussed herein will be made; the result should be useful for future comparison with the effectiveness of other vanes and blades to be tested.

Application to vane. - The correlation equations derived in appendix B and discussed briefly in the preceding sections of this report may be used in several ways. One application is to the midspan section of the vane, where average values are considered for each of the variables. A second application considers the correlation of data at local positions at the midspan on the vane. Both applications are discussed in the following paragraphs.

To apply the correlations, average values of T_{ge} and T_w are used to determine an average φ. The value of $\overline{T}_{ge}$ for this purpose may be selected either as the midspan turbine inlet gas temperature $T_{T,i}$ to the vane or as the integrated average of the local values of T_{ge} at the midspan. The difference between the integrated average of the local values of T_{ge} and the value of the midspan turbine inlet temperature was found to be only about 14 K (25° F). For ease in calculation, the value of $T_{T,i}$ was therefore used in the calculations herein, both for $\overline{T}_{ge}$ and for the basis of gas property values.

The integrated average value of the local corrected vane wall temperatures is used for $\overline{T}_w$. Because the cascade walls were water cooled, significant radiative heat losses from the vanes to the walls occurred. In order to account for these losses, the measured vane wall temperatures were corrected by use of the method described in reference 16. Throughout this report, T_w is the corrected wall temperature and $\overline{T}_w$ the integrated average of the corrected wall temperatures. An average value of the cooling-air temperature should also be used. However, the correlation was attempted with the use of the inlet coolant temperature $T_{c,i}$ both in determination of $\overline{\varphi}$ and in the evaluation of the cooling-air property values, since $T_{c,i}$ is usually well known and is a logical reference temperature. Total coolant flow and total gas flow was also used.

To apply the correlation equation to a local position on the vane, φ was based on the inlet gas temperature to the vane $T_{T,i}$, the local wall temperature T_w, and the coolant inlet temperature $T_{c,i}$.

Determination of exponents in correlations. - The correlation equations discussed previously contain powers of the gas flow, coolant flow, and film-cooling flow rates. A brief discussion of how these exponents were determined follows.

The exponent m was determined as the slope of the line (or lines) through the data plotted with Y as ordinate, $(\dot{w}/\mu)_c$ as abscissa, and $(\dot{w}/\mu)_g$ as parameter on log-log scale. By crossplotting the data (i.e., $Y(\dot{w}/\mu)_c^m$ as ordinate and $(\dot{w}/\mu)_g$ as abscissa), the slope of the line through the data determined the exponent n.

A similar procedure was followed for application of the correlation equations for local positions. New values of m and n were required. The new values were determined as before, except that local values of Y were used.

Predicted Wall Temperatures

The flow characteristics of the coolant as it passes through the vane internal cooling passages must be known in order to predict vane wall temperatures. To determine these flow characteristics, a one-dimensional compressible flow network simulation of the internal cooling configuration was used. Experimentally measured pressures and flow distributions (ref. 4) for the vane of figure 4 were required to determine the inlet and exit losses, the friction pressure drops, and the coefficients for the one-dimensional flow network.

With the flow coefficients as determined by experimental data from the flow facility available, the flow distribution through the vane in the cascade was determined. The pressures at each coolant exit location were obtained from either a measured or a calculated pressure distribution around the vane profile. By using pressures from figure 13 of reference 9, the measured leading-edge exit pressure, and the measured total coolant flow rate and inlet temperature, the flow distribution through the vane was determined by analytically varying the inlet pressure until the calculated total flow equals the measured total flow. An alternate way of determining the flow distribution was to set the inlet pressure equal to the measured inlet pressure and calculate the flow. The first method was used since the correct value of total flow rather than the correct inlet pressure was preferred. If the one-dimensional compressible flow network simulation represented the vane perfectly, identical results would be obtained using either method.

For the prediction of vane wall temperatures, a number of other quantities must be known. External to the vane, the effective gas temperature distribution and the convective gas-to-vane heat-transfer coefficients must be available. The effective gas temperature can be obtained by use of equation (4), and the convective gas-to-vane heat-transfer coefficients can be found for the vane leading edge by use of equation (1) and for the vane midchord region by use of equation (2). For the film-cooled vane trailing edge, the film-cooling effectiveness and the adiabatic wall temperature are required. The film-cooling effectiveness can be obtained from equation (5).

To complete the heat-transfer analysis and calculate vane temperatures, the internal heat-transfer coefficients must also be known. For the impingement-cooled leading edge, the correlation of reference 17 was used. For the vane under consideration, the correlation for the average heat-transfer coefficient over the leading-edge node reduced to

$$\overline{h}_{c,le} = 0.06549\left(Re_{c,le}^{0.7}\right)\frac{k_c}{b} \tag{12}$$

where

$$Re_{c,le} = \frac{\dot{w}}{A}\frac{b}{\mu}$$

and where $\dot{w}$ is the flow rate per hole and b is the equivalent slot width. For the midchord region, the impingement correlation of reference 18 was used; it is

$$\bar{h}_{c,mc} = 0.286\, Re_a^{0.625}\frac{k_c}{c_n} \tag{13}$$

where

$$Re_{a,mc} = \frac{v_a c_n \rho}{\mu}$$

(Since $z_n/D < 6$, the arrival velocity equals the nozzle exit velocity, i.e., $v_a = v_n$.) For the split trailing edge, the pin fin correlation of reference 19 was used; it is

$$h_{c,te} = 0.248\, Re_{c,te}^{0.594}\, Pr_c^{0.333}\frac{k_c}{d} \tag{14}$$

where

$$Re_{c,te} = \frac{v_c d \rho}{\mu}$$

and d is the pin fin diameter.

For the heat-transfer calculations, a nodal network for the vane wall, including the pin fins, was established. Assumed initial vane wall temperatures must be used to determine gas-to-vane heat-transfer coefficients. Then the combined flow and heat-transfer programs were used, with the known flow characteristics as described previously, to determine the vane temperatures. Iteration between flow and heat transfer was required until the calculated vane temperatures converged and the total calculated flow converged to the measured total flow.

Comparison of Measured and Calculated Flow Distributions

The combined flow and heat-transfer calculation procedure determined local values of the coolant flow through individual regions of the vane. These values were compared with measured values of the flow through the same vane regions. The measured flows were obtained from the experimental pressures measured in the coolant passages during the cascade tests and from use of the correlations of reference 5.

RESULTS AND DISCUSSION

Gas Temperature and Gas-to-Wall Heat-Transfer Coefficient Profiles

As noted previously, since tests were made over a range of gas temperatures from 700 to 1644 K (800° to 2500° F), two different burners were used: one for high-gas-temperature runs, and the other for low-gas-temperature runs. Figure 6 shows the spanwise total inlet gas temperature profiles for the two burners; the upper curve on figure 6 is the spanwise profile for the high-temperature burner for a nominal gas temperature of 1644 K (2500° F). The lower two curves compare the profiles for the two

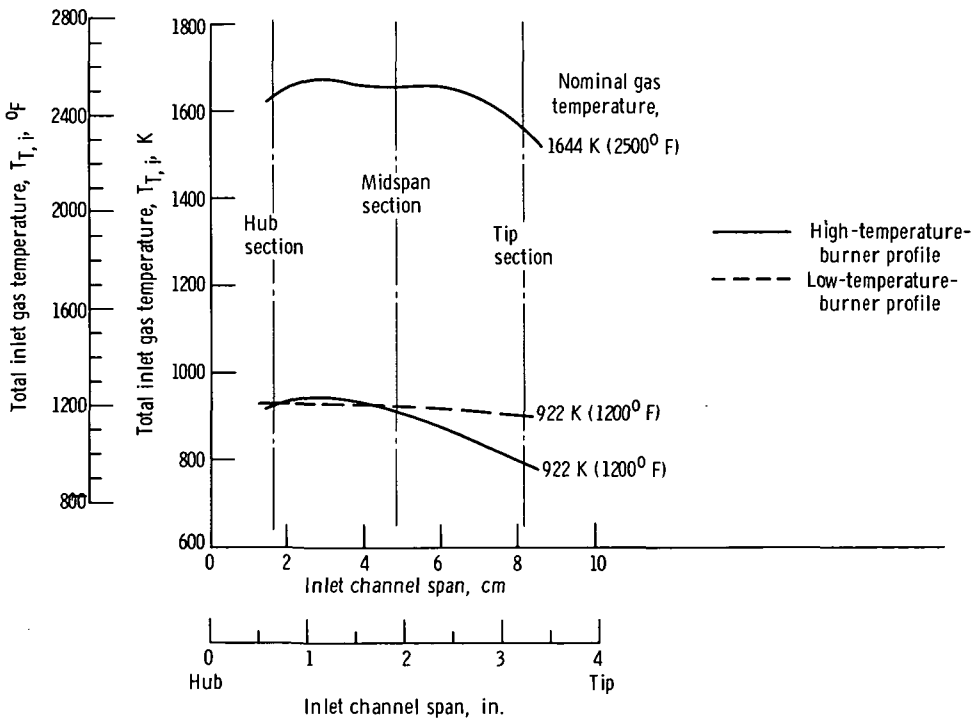

Figure 6. - Typical combustion gas total inlet temperature profiles for high- and low- temperature burners.

burners for a nominal gas temperature of 922 K (1200° F).

The ratios of maximum to average temperature over the area scanned were 1.025 and 1.051 for the high-temperature burner for 1644 K (2500° F) and 922 K (1200° F), respectively. For the low-temperature burner the ratio was 1.011. Superimposed on the temperature profiles are the approximate locations (hub, midspan, and tip sections) of the thermocouples on the test vanes. The nominal 922 K (1200° F) gas profile for the high-temperature burner was skewed to the hub section and the high- and low-temperature burner profiles differed by approximately 110 K (200° F) at the tip section. This could result in a considerable change in the conductive heat loss from the vane and therefore affect the heat-transfer characteristics at the midspan.

Figure 7 is a representative plot of the chordwise distribution of the effective gas temperature for the high-temperature burner operating at a nominal temperature of 1644 K (2500° F). The distributions around the hub, midspan, and tip sections of the vane are shown in the figure. These distributions were obtained by use of equation (4). Similar distributions were also found for other operating conditions, but are not presented. A comparison of the midspan value of the total inlet gas temperature for the high-temperature burner (fig. 6) with either the leading-edge or average midspan value of the effective gas temperature (fig. 7) shows negligible difference. Consequently, for ease in calculation, the value of the midspan total inlet temperature was used instead of the effective gas temperature in the correlations to be presented.

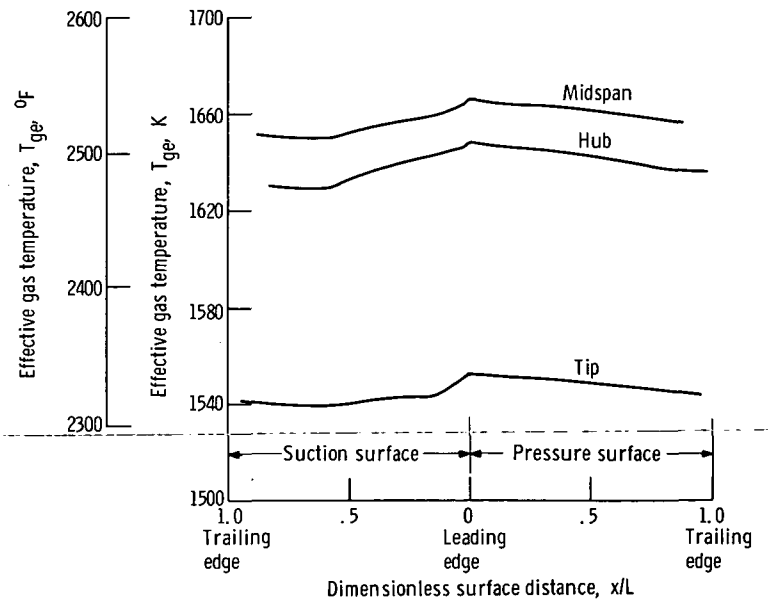

Figure 7. - Representative plot of effective gas temperature for high-temperature burner operating at nominal gas temperature of 1644 K (2500° F).

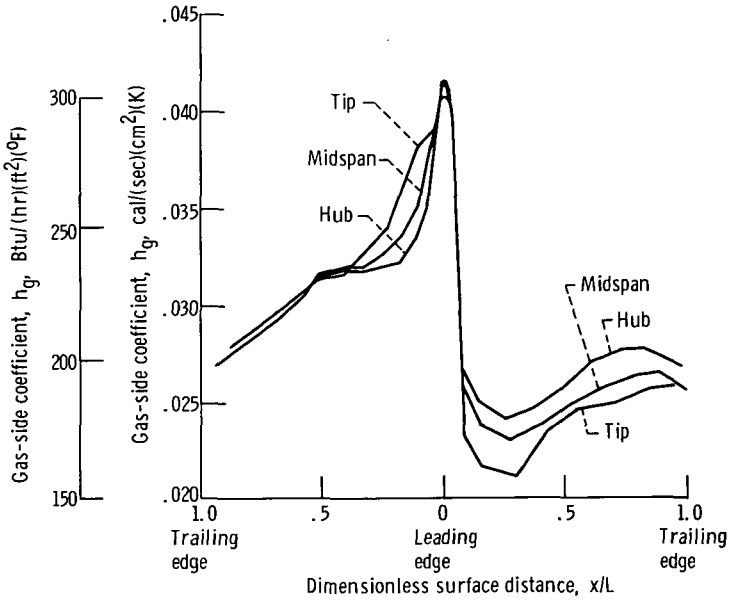

Figure 8. - Representative plot of gas-side heat-transfer coefficient for high-temperature burner operating at nominal gas temperature of 1644 K (2500° F).

Figure 8 shows a representative chordwise distribution of the convective gas-to-vane heat-transfer coefficients for a nominal gas temperature and pressure of 1644 K (2500° F) and 31 N/cm^2 (45 psia), respectively. The distributions around the hub, midspan, and tip sections are presented. These distributions were obtained by use of equations (1) and (2); equation (1) applies to the vane leading-edge region, and equation (2) to the remainder of the vane. Similar distributions were obtained for other nominal gas temperatures.

Determination of Average and Local Vane Temperatures

Thermocouples were placed in duplicate locations on the two test vanes. The following procedure was used for obtaining temperatures to use in the heat-transfer correlations. The integrated average midspan temperatures were found for each vane; these were then averaged arithmetically to obtain $\overline{T}_w$. Local vane temperatures were obtained by arithmetically averaging the temperatures at similar thermocouple locations of the two test vanes.

Correlation of Average Midspan Temperatures

A correlation of average midspan temperatures is an indication of the overall effectiveness of the cooling air used; however, this type of correlation does not reflect

local hot spots. Therefore, the correlation of local temperatures is discussed after the average correlation. The evaluation of $\overline{\varphi}$ required in each of the correlations to be discussed was based on the average midspan temperature $\overline{T}_w$, the inlet coolant temperature $T_{c,i}$, and the total midspan turbine inlet temperature $T_{T,i}$. Property values were based on coolant inlet and midspan turbine total inlet temperatures and were evaluated by use of reference 20. Data for gas temperatures of 700, 811, 922, and 1644 K (800°, 1000°, 1200°, and 2500° F) and coolant temperatures of 292, 300, 456, and 589 K (65°, 80°, 360°, and 600° F) and for coolant flow ratios from 0.02 to 0.15 were used for the correlations. A common set of symbols for distinguishing the data points were used throughout; they are defined in table II. All correlation equations were obtained by least-squares curve fit.

$\overline{Y}$ correlation. - In order to make use of the correlation equation it was necessary to determine the values of the exponents m and n for the quantities $(\dot{w}/\mu)_c$ and $(\dot{w}/\mu)_g$. To determine the exponent m, a plot of $\overline{Y}$ against $(\dot{w}/\mu)_c$ was made for all the data on log-log scale. This is shown in figure 9. For each value of the parameter $(\dot{w}/\mu)_g$ in figure 9, a correlating line was determined. Two typical correlating lines are shown in the figure. The slopes of these lines were then arithmetically averaged. This value was found to be -0.85. The exponent n was then found by plotting, on a log-log scale,

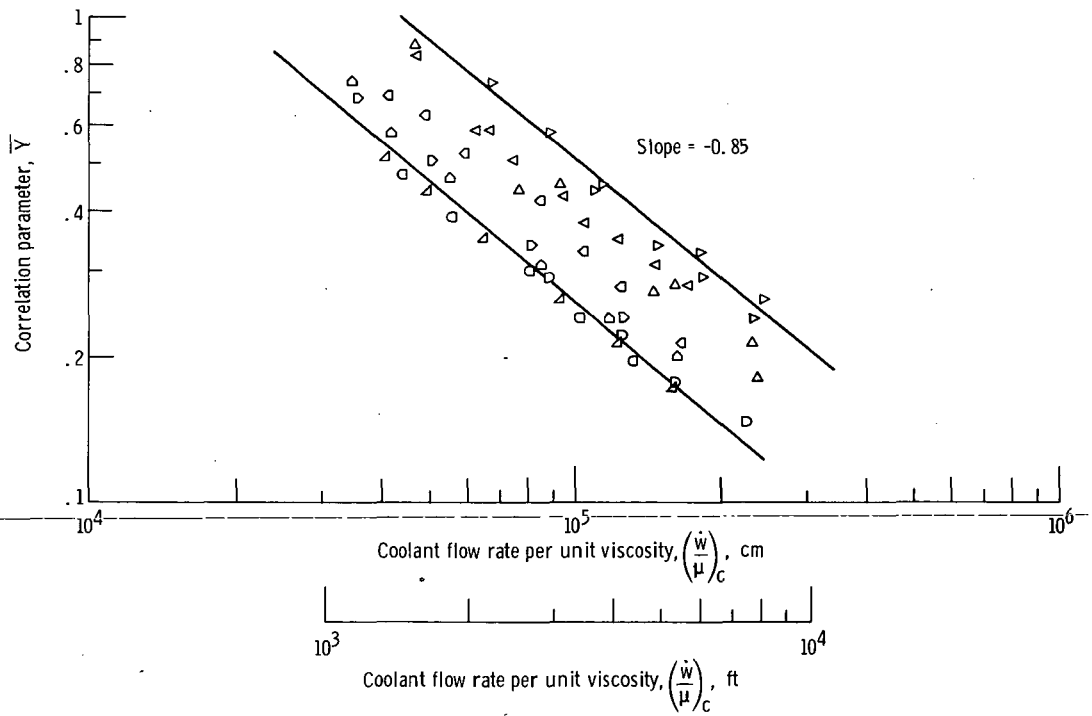

Figure 9. - Representative figure showing determination of m. (See table II for symbol definition.)

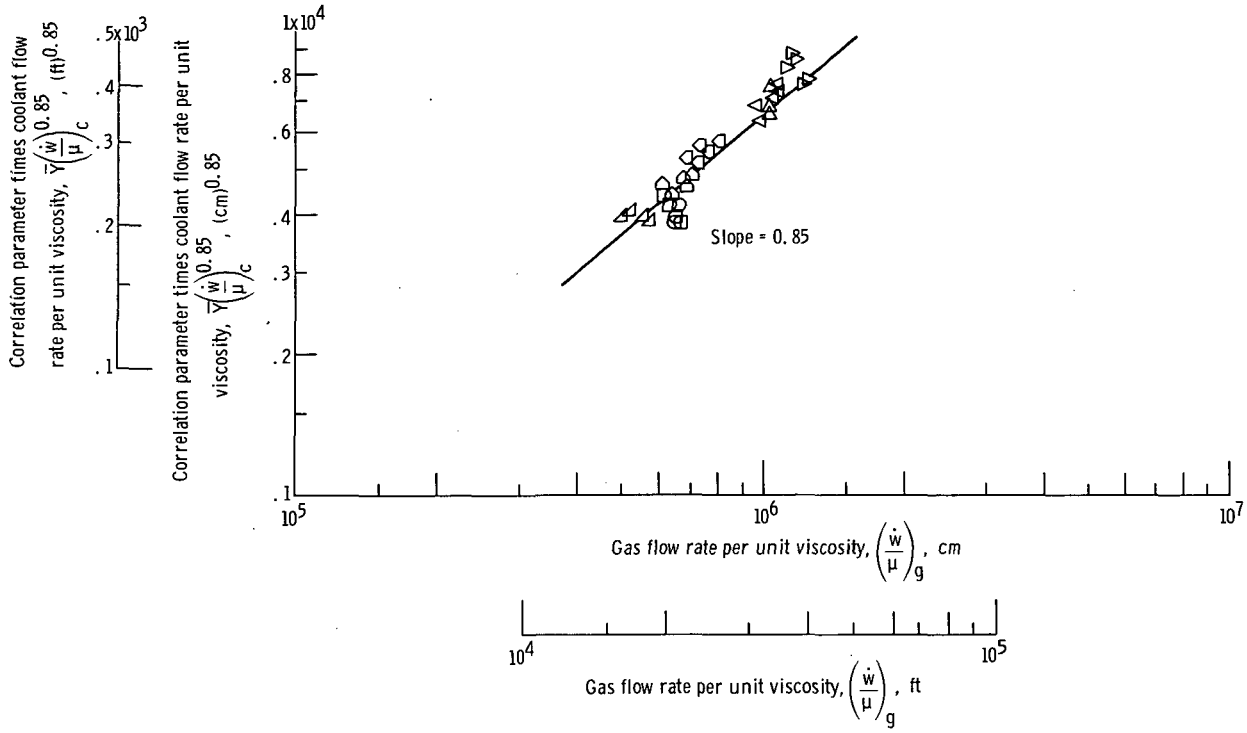

Figure 10. - Representative figure showing determination of n. (See table II for symbol definition.)

the product $\overline{Y}(\dot{w}/\mu)_c^{0.85}$ against $(\dot{w}/\mu)_g$. This plot is shown in figure 10; a line through the data yielded a value of 0.85 for the exponent n.

With the values of m and n now known, the data were plotted with $\overline{Y}$ as ordinate and

$$\left(\frac{\dot{w}}{\mu}\right)_g^{0.85} \Big/ \left(\frac{\dot{w}}{\mu}\right)_c^{0.85}$$

as abscissa (fig. 11). The line through the data is given by

$$\overline{Y} = 0.059\left[\left(\frac{\dot{w}}{\mu}\right)_g \Big/ \left(\frac{\dot{w}}{\mu}\right)_c\right]^{0.85}$$

The figure indicates an increased scatter in the data with decreasing coolant flow. Shown on the figure is a ±15 percent scatter band. The effect of this scatter on the airfoil temperature as measured and as calculated by the equation is discussed in the section Comparison of Average Measured Temperatures with Average Temperatures Obtained from the Correlations.

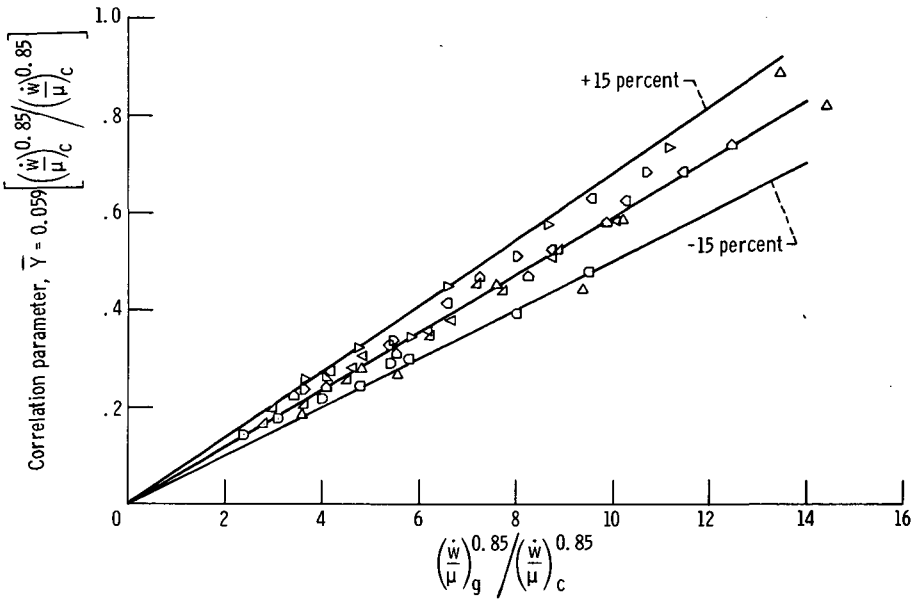

Figure 11. - Correlation of average midspan data, using equation (B12). (See table II for symbol definition.)

A similar set of calculations were made to investigate the use of the simplified correlation, equation (7), from which all property values have been deleted. Results similar to those found for the $\overline{Y}$ correlation were obtained.

$\overline{\varphi}$ correlation. - The simplest correlation is obtained by plotting $\overline{\varphi}$ against the flow parameter $\dot{w}_c/\dot{w}_g$. Since $\dot{w}_c$ represents the total coolant flow and $\dot{w}_g$ the total gas flow, the ordinate (coolant flow ratio or dilution) is always known (from heat-transfer tests or for design considerations) and the simplified correlation is of more universal value. The correlation is shown in figure 12. A curve through the data is also shown; it is

$$\overline{\varphi} = \frac{1}{1 + 0.082\left(\frac{\dot{w}_g}{\dot{w}_c}\right)^{0.80}} \tag{14}$$

The maximum deviation from the curve was calculated as ±4 percent for $\dot{w}_c/\dot{w}_g = 0.04$ and ±8 percent for $\dot{w}_c/\dot{w}_g = 0.10$. The effect of these deviations on vane wall temperatures is discussed in the section Comparison of Average Measured Temperatures with Average Temperatures Obtained from the Correlations.

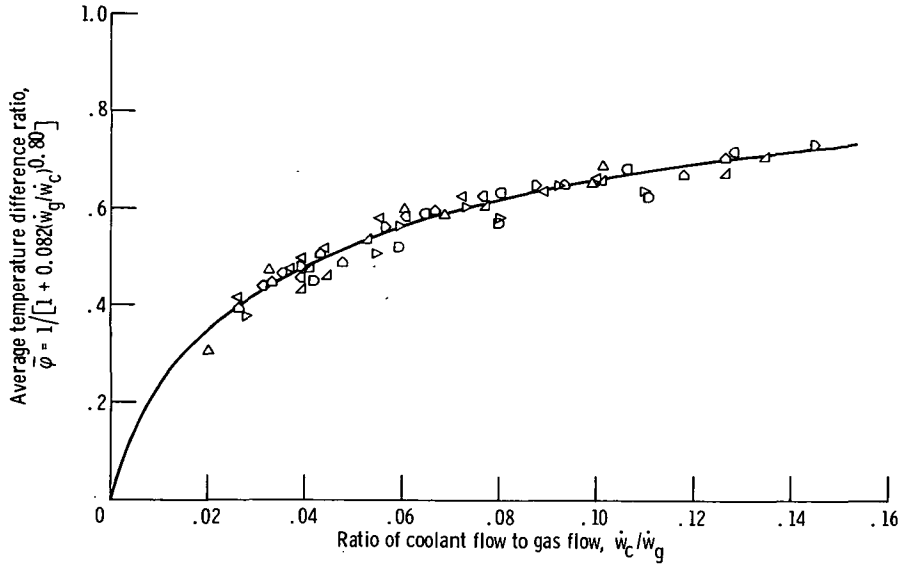

Figure 12. - Average temperature difference ratio for midspan against ratio of coolant flow to gas flow. (See table II for symbol definition.)

Correlation of Local Midspan Temperatures

The methods used to correlate the average midspan vane temperature data may also be used to correlate local temperature data. The correlations are based on local measured temperatures, the turbine inlet temperature, the coolant inlet temperature, and properties associated with the latter two temperatures. Total inlet flow rates were also used.

Y_x correlation. - The exponents m and n for the two terms $(\dot{w}/\mu)_c$ and $(\dot{w}/\mu)_g$ in equation (B12) were determined for each individual thermocouple location in the same manner as was done for average values of Y. Plots of Y against

$$\left(\frac{\dot{w}}{\mu}\right)_g^n \Big/ \left(\frac{\dot{w}}{\mu}\right)_c^m$$

for four representative thermocouples are shown in figure 13; the common symbol set is used for the local correlation data plots. The four representative thermocouples chosen are thermocouples 12, 9, 8, and 4 (fig. 5(a)); the Y_x correlations for these thermocouples are shown in figures 13(a) to (d), respectively. An equation for each of these correlations is shown in the respective figure legend. The ratio of coolant flow rate to gas flow rate varied from approximately 0.02 to 0.15.

Correlation of data using equation (B10) was also attempted. To use this equation, the outlet coolant temperature $T_{c,s}$ must be known. Also, an accurate expression for

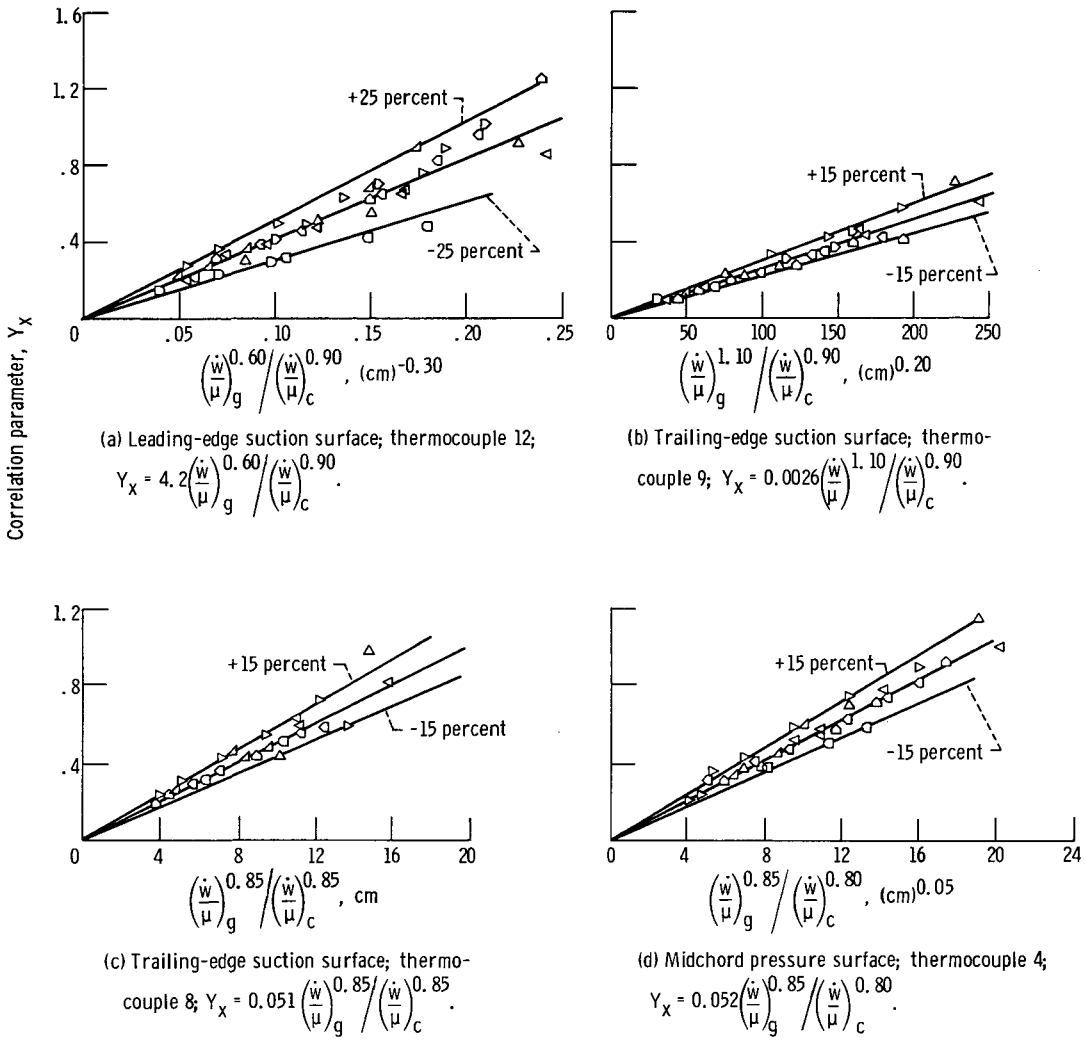

Figure 13. - Local Y_X correlation of selected midspan thermocouples. (See table II for symbol definition.)

η_f must be available. Since there were no thermocouples measuring the outlet coolant temperatures and since a film-cooling correlation accurately representing the vane slot geometry did not exist, it was impossible to achieve better correlation of data than that obtained by using equation (B12). An attempt was made to correlate the data by using a calculated $T_{c,s}$, with no improvement in the results.

The data scatter is attributed in part to the use of a coolant inlet temperature instead of the local coolant temperature. As the coolant flow decreases, the temperature rise of the coolant becomes greater and, consequently, the inlet temperature becomes less representative of the local coolant temperature. Some data scatter may also be attributed to the fact that total gas and total coolant flows were used.

Shown in figure 13 are scatter bands of ±15 percent, except for figure 13(a) which has ±25 percent scatter bands.

The exponents shown in figure 13 range in value from 1.10 to 0.60, but with most of the values between 0.80 and 0.90. The exponent values, 1.10 and 0.60, are on the gas-side flow parameter and represent temperature data immediately downstream of the suction surface film-cooling slot and a point on the suction surface leading edge, respectively. The latter point may be in either a laminar or transition flow regime. The two remaining exponents on the gas-side flow parameter are equal to 0.85, which is slightly higher than the turbulent flow exponent of Reynolds number of 0.80. The exponents on the coolant-side flow parameter are, for figures 13(a) and (b), respectively, 0.90, 0.90, 0.85, and 0.80. The first two exponents were determined for a pin-fin-cooled regime of the leading edge and for the region at the end of the impingement-cooled midchord and the beginning of the pin-fin-cooled trailing edge, respectively. The latter two exponents were determined for the pin-fin-cooled trailing edge and for the beginning of the impingement-cooled midchord region, respectively. The exponents of 1.10 and 0.60 on the gas-side flow parameter would be expected to deviate from 0.80. However, the other exponents would be expected to be 0.80. The reasons for the deviation from this value are not clearly understood and further investigation is in order.

φ_x correlation. - Figure 14 shows the local temperature difference ratio φ_x as a function of the ratio of coolant to gas flow for the same thermocouple locations considered in figure 13. As would be expected, the thermocouples affected by film cooling give a higher value of φ_x for a given value of $\dot{w}_c/\dot{w}_g$ than do the thermocouples not affected by film cooling. The maximum deviation of the data from the correlation curves was found to be ±25 percent for a $\dot{w}_c/\dot{w}_g$ ratio of 0.04 and ±10 percent for a $\dot{w}_c/\dot{w}_g$ ratio of 0.10 for figure 14(a). Figures 14(b) to (d) show maximum deviations of ±10 percent for $\dot{w}_c/\dot{w}_g$ ratios of 0.04 and 0.10. These figures also give the correlation equations for the respective locations. Table III gives the correlation equations for all 13 local midspan thermocouple locations.

Effect of Spanwise and Chordwise Temperature Gradients on the Correlations

The correlations presented herein were developed from one-dimensional heat flow considerations. Deviation from the one-dimensional model will affect correlations and, in general, conduction effects will alter the measured airfoil temperature and therefore the value of φ. For the data presented, the maximum ratio of heat lost by spanwise and chordwise conduction to the total heat transferred to the vane from the gas stream was approximately 0.15. This maximum value occurred at a high coolant flow ratio (approximately 0.10) and a turbine inlet temperature of 1644 K (2500° F).

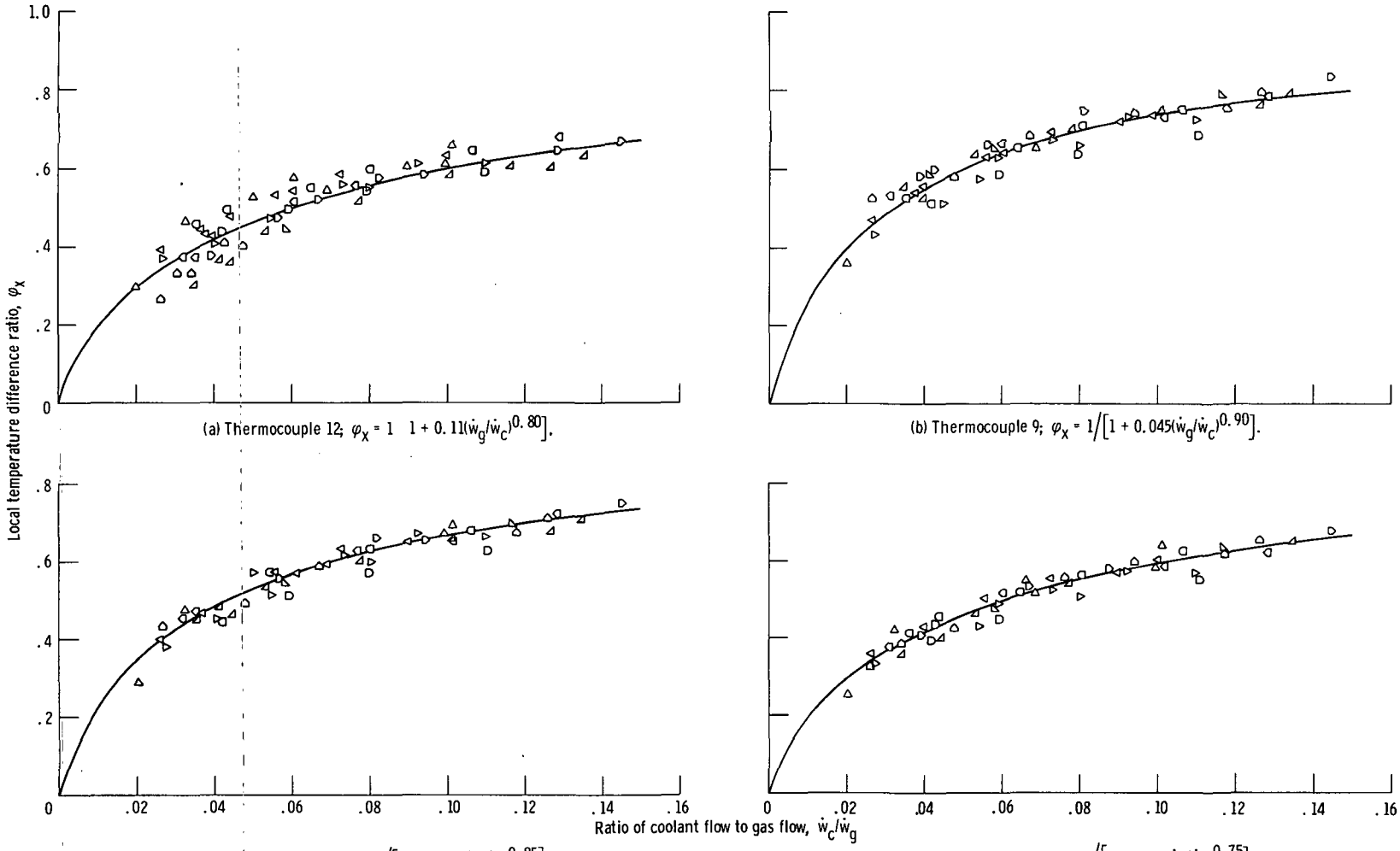

(a) Thermocouple 12; $\varphi_x = 1 \quad 1 + 0.11(\dot{w}_g/\dot{w}_c)^{0.80}]$.

(b) Thermocouple 9; $\varphi_x = 1/[1 + 0.045(\dot{w}_g/\dot{w}_c)^{0.90}]$.

(c) Thermocouple 8; $\varphi_x = 1/[1 + 0.071(\dot{w}_g/\dot{w}_c)^{0.85}]$.

(d) Thermocouple 4; $\varphi_x = 1/[1 + 0.12(\dot{w}_g/\dot{w}_c)^{0.75}]$.

Figure 14. - Local temperature difference ratio as function of the ratio of coolant flow to gas flow at midspan. (See table II for symbol definition.)

TABLE III. - LOCAL TEMPERATURE DIFFERENCE EQUATIONS FOR MIDSPAN THERMOCOUPLE POSITIONS

$$\varphi_x = \frac{1}{1 + E\left(\frac{\dot{w}_g}{\dot{w}_c}\right)^F}$$

Thermocouple	E	F
1	0.12	0.75
2	.10	.80
3	.075	.90
4	.12	.75
5	.058	.90
6	.017	1.20
7	.053	.95
8	.071	.85
9	.045	.90
10	.11	.60
11	.13	.70
12	.11	.80
13	.10	.75

Comparison of Average Measured Temperatures with Average Temperatures Obtained from the Correlations

The vane average midspan temperatures obtained from averaging local measured midspan temperatures were compared with average midspan temperatures calculated by use of the average correlation equations. The results are presented in figures 15 and 16 for the $\overline{Y}$ and $\overline{\varphi}$ correlations, respectively. All the cases considered in the investigation are represented in these figures. Five-percent error bands are also shown in the figures. Inspection of the figures shows that the $\overline{Y}$ correlation calculations exceeded the measured values in more cases than did the $\overline{\varphi}$ correlation calculations. Because of this, and because of the greater ease in application of the $\overline{\varphi}$ correlation, the $\overline{\varphi}$ correlation should be used for estimating average metal temperatures for this vane. In addition to its ease in application, the $\overline{\varphi}$ correlation also serves as a good measure for comparing the average cooling effectiveness of different cooling configurations.

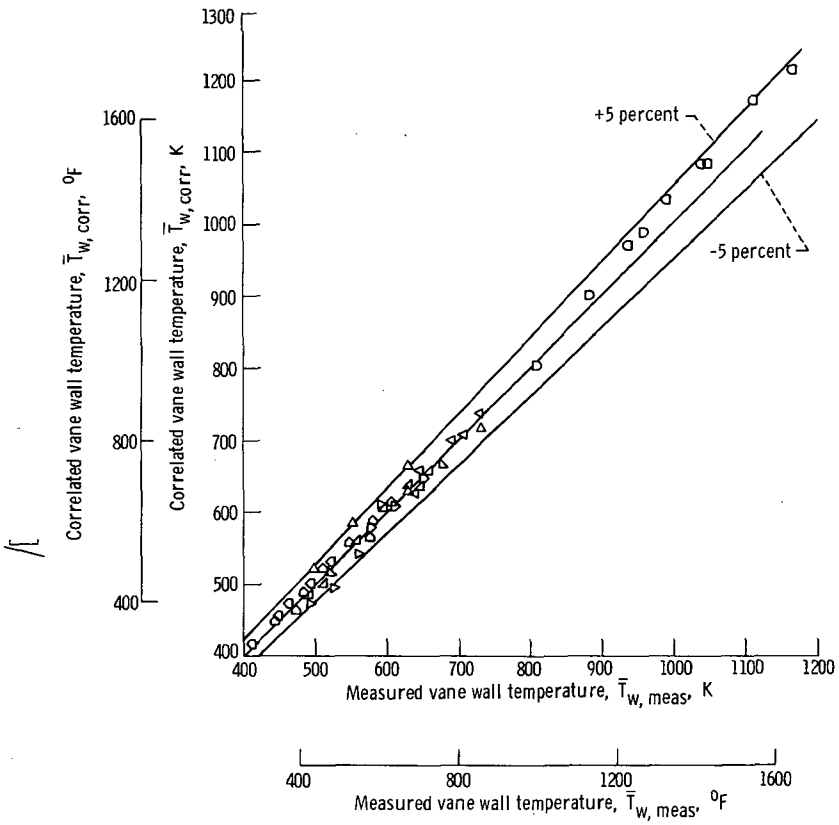

Figure 15. - Comparison of average measured midspan temperature with average temperature calculated from $\bar{Y}$ correlation. (See table II for symbol definition.)

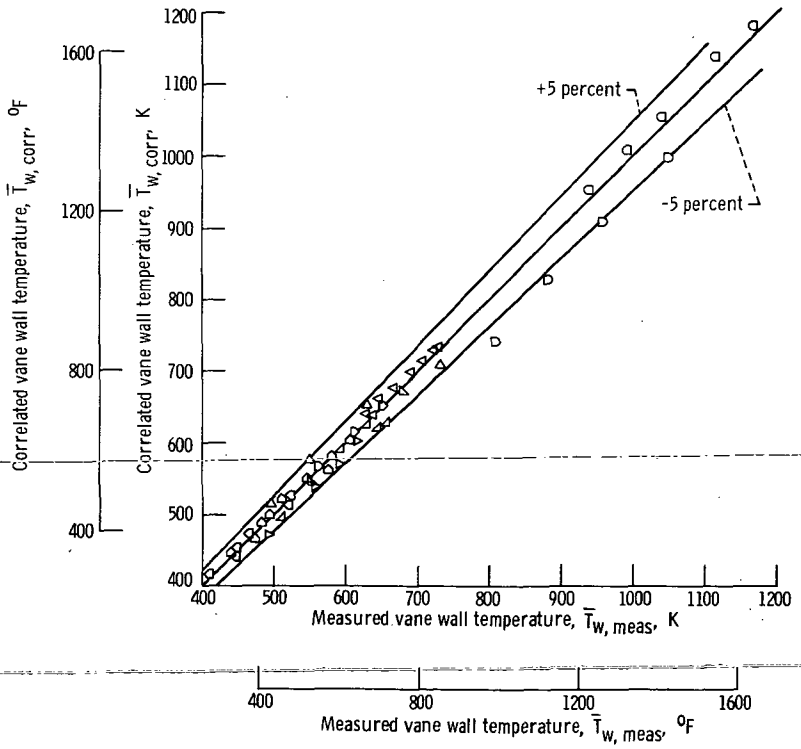

Figure 16. - Comparison of average measured midspan vane temperature with average temperature calculated from $\bar{\varphi}$ correlation. (See table II for symbol definition.)

Comparison of Local Midspan Measured Vane Temperatures with Local Temperatures Obtained from the Correlations

Local midspan vane temperatures $T_{w,x}$ were calculated from local Y and local φ correlations for the representative thermocouples 12, 9, 8, and 4 (fig. 5(a)). The resultant error in calculating these local temperatures was greater than the error of 5 percent found in calculated average vane midspan temperatures (fig. 16). The maximum error for calculated local temperatures was 16 percent. However, the majority of calculated local temperatures had errors smaller than 16 percent.

Since the majority of the runs reported herein yield data closer to the correlation curves than ±16 percent, it can be concluded that the calculated values of $T_{w,x}$ will in general be much closer to the measured values of $T_{w,x}$ for most cases. However, since the φ_x correlation is so easy to apply, and since in most cases it is as accurate as the Y_x correlation, it appears that satisfactory estimates of local vane temperatures can be obtained by use of the φ_x correlation. It must be noted again that lack of a measured coolant temperature at the vane midspan position resulted in the use of the coolant inlet temperature for evaluating coolant properties. This undoubtedly affects the local vane temperatures as calculated from the Y_x correlation. The suggestion to use the φ_x correlation for estimating vane local temperatures eliminates the necessity of evaluating property values and of determining the exponents m and n for each thermocouple location, and yet yields satisfactory estimates of the vane local temperatures.

Comparison of Calculated and Measured Flows

The ability to calculate coolant flow distributions is of prime importance when designing a vane or blade to meet advanced engine requirements.

The coolant flow discharged at the four major exit points (the leading edge, the suction and pressure surface film-cooling slots, and the split trailing edge) was determined by use of measured internal pressures, the gas stream static pressure found in reference 9, and the empirical flow results of reference 4. The four individual flows were then normalized to the total measured coolant flow into the vane. The results are compared in figure 17 to the flow distribution calculated by the analytical program described previously.

Figures 17(a) to (d) show a comparison for the trailing edge, the suction surface film-cooling slot, the leading edge, and the pressure surface film-cooling slot. The leading-edge flow compares quite favorably, with the greatest difference at the high flow

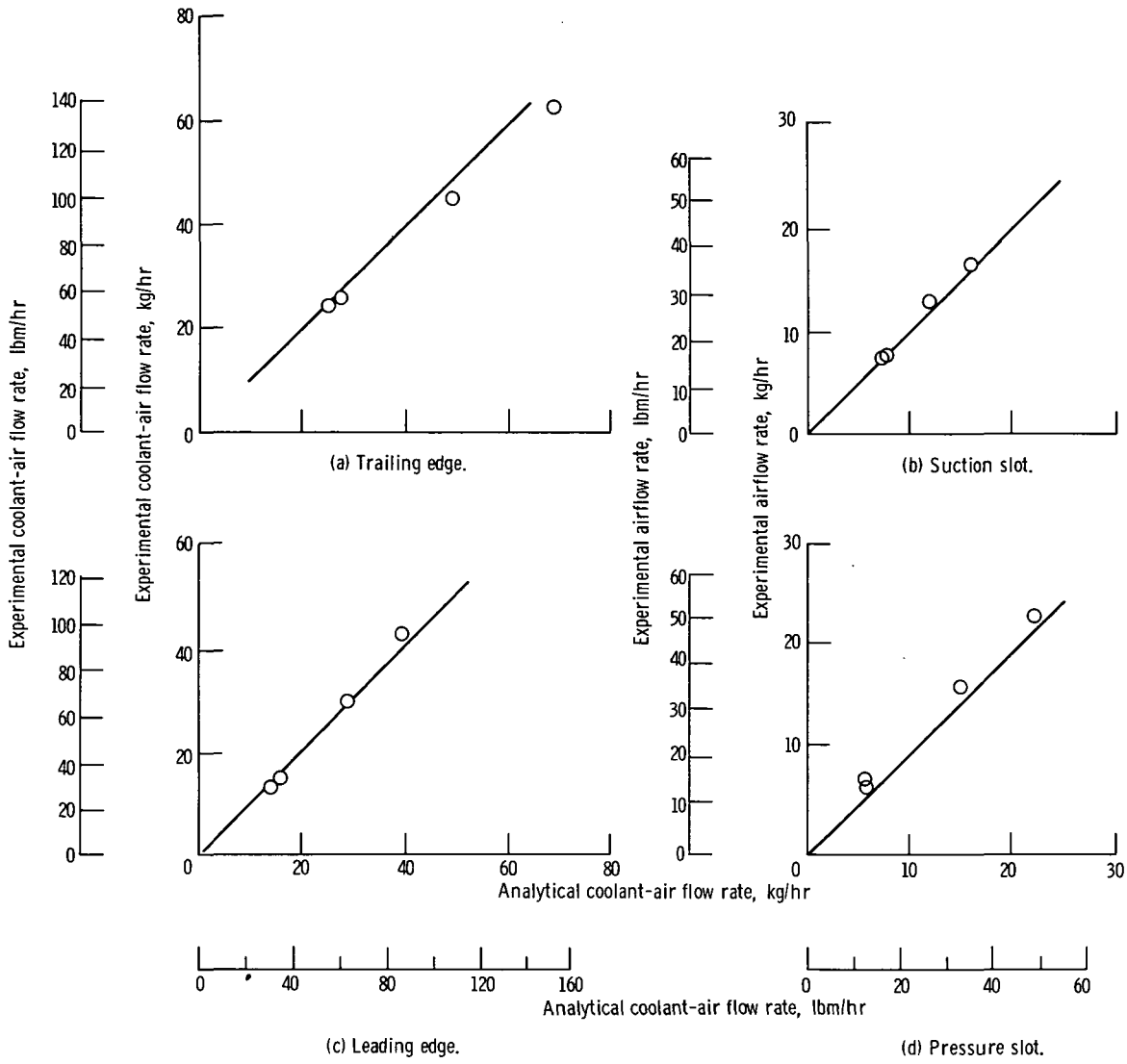

Figure 17. - Comparison of experimental coolant flow determined by use of reference 4 with an analytically determined coolant flow.

point, and was approximately 6 percent high. For the trailing edge, the empirical flow is approximately 8 percent or less lower than the analytical flow.

Comparison of Predicted and Measured Vane Wall Temperatures

The ability to calculate vane temperatures is also of prime importance when designing a vane or blade to meet advanced engine requirements.

Experimental and predicted local vane temperatures for the midspan location are presented in figures 18(a) to (d) for turbine inlet and coolant inlet temperatures of 916

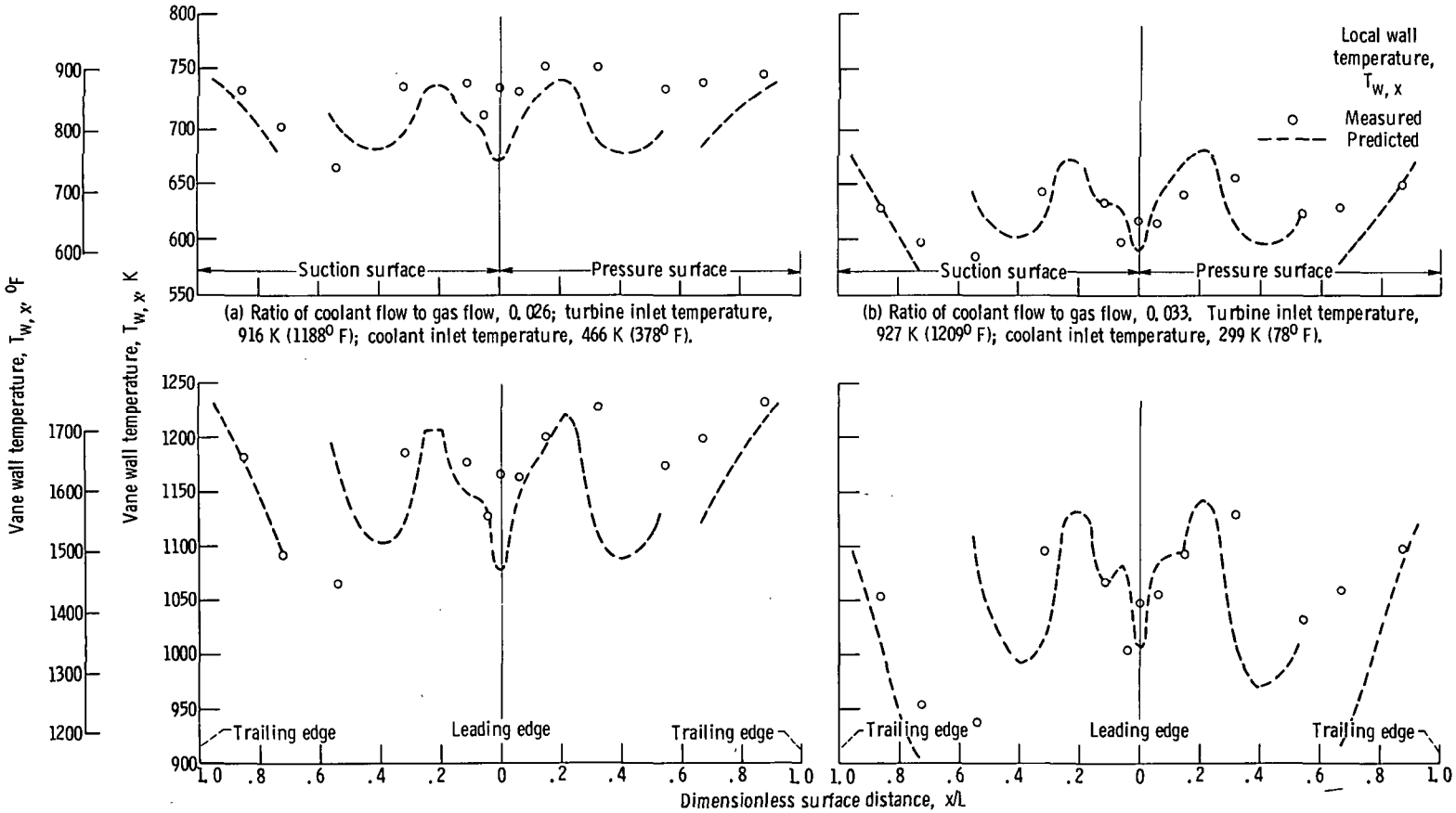

(a) Ratio of coolant flow to gas flow, 0.026; turbine inlet temperature, 916 K (1188° F); coolant inlet temperature, 466 K (378° F).

(b) Ratio of coolant flow to gas flow, 0.033. Turbine inlet temperature, 927 K (1209° F); coolant inlet temperature, 299 K (78° F).

(c) Ratio of coolant flow to gas flow, 0.035; turbine inlet temperature, 1644 K (2500° F); coolant inlet temperature, 589 K (600° F).

(d) Ratio of coolant flow to gas flow, 0.042; turbine inlet temperature, 1644 K (2500° F); coolant inlet temperature, 298 K (76° F).

Figure 18. - Comparison of measured and analytical vane wall temperatures at midspan.

and 466 K (1188° and 378° F), 927 and 299 K (1209° and 78° F), 1644 and 589 K (2500° and 600° F), and 1644 and 298 K (2500° and 76° F), respectively. The ratios of coolant flow to gas flow were 0.026, 0.033, 0.035, and 0.042, respectively.

In general, the maximum percent error in predicting the local vane temperatures increases for increasing difference between $T_{T,i}$ and $T_{c,i}$. Figures 18(a) to (d) show percent errors of ±7.5, ±7.5, ±9.1, and ±15.2, respectively. The maximum errors which occur are usually at thermocouples 6 and 10 (fig. 5(a)).

Figure 18 shows that the predicted temperatures are best in regions of convection cooling. In the portions of the vane where impingement cooling and film cooling are predominant, the predicted temperatures are not as good. This result is to be expected though, since for these two modes of cooling, surface and slot geometries are important and correlations did not exist for geometries exactly matching the airfoil's particular geometry.

A possible source of error between predicted and measured temperatures is the positioning of thermocouples behind slots grooved for other thermocouple positions (fig. 5(b)). During testing, the ceramic in the slots bubbled up and could have acted as a turbulator, increasing turbulence and heat transfer to the vane.

Cooling Effectiveness

The cooling effectiveness of a vane can be described by equation (9). A plot of φ against η_t is a means for comparing the effectiveness of different vanes. An attempt to correlate the data on a plot of φ against η_t failed because the $T_{c,o}$ needed in equation (10) was not measured experimentally.

Therefore a sample calculation of the thermal effectiveness as given by equation (9) was made for a turbine inlet temperature of 1644 K (2500° F), an inlet cooling-air temperature of 589 K (600° F), and a coolant- to gas-flow ratio of 0.035. The average discharge temperature $T_{c,o}$ was determined from a weighted average of the temperatures of the outlet coolant flows found by the computer program which was used to predict vane temperatures. Values for φ and $\overline{T}_w$ for use in equations (9) and (10) were obtained from the correlation equation for $\overline{\varphi}$ (fig. 12), using the conditions listed. The thermal effectiveness η_t was 0.58 and φ was 0.46.

Vane Operating Potentialities

The operating limits of the vane investigated are discussed in the following paragraphs.

$T_{w,max}$ against $\overline{T}_w$. - Ideally, the maximum and the average vane temperatures should be equal, indicating that the coolant flow is ideally distributed. However, practically, a difference will exist between the maximum and the average vane temperature and this difference will represent the degree of maldistribution of coolant flow. Figure 19 is presented to show the relationship between the maximum and average metal temperature for the vane investigated. For an extrapolated maximum vane temperature of 1311 K (1900° F) the average temperature will be approximately 1255 K (1800° F), which for practical application, represents a good coolant flow distribution. This maximum temperature occurred at thermocouple position 4 for nearly all data points taken. For the few exceptions, the temperature of thermocouple positions 3 exceeded that of position 4 by as much as 11 K (20° F)(see fig. 5(a)).

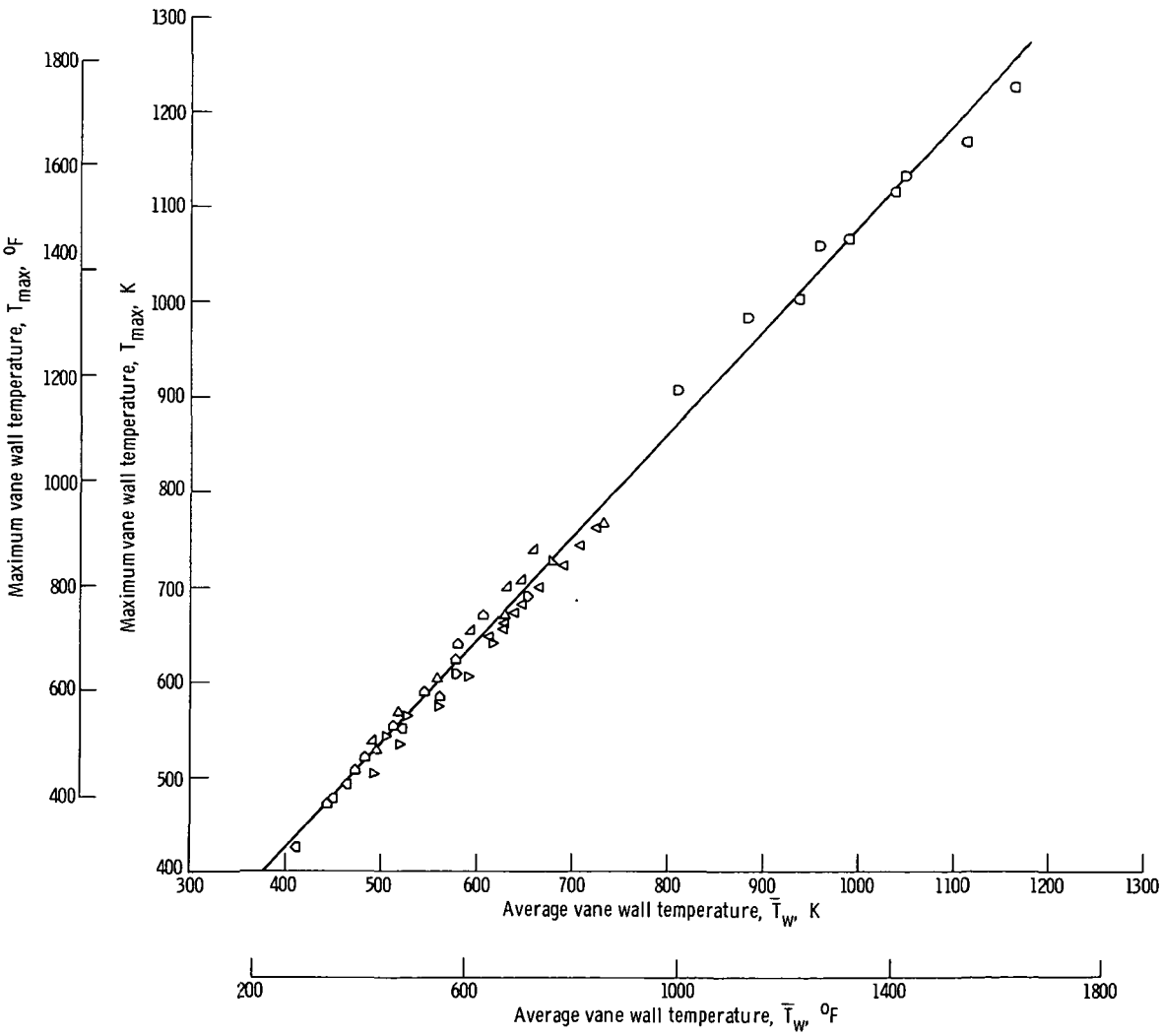

Figure 19. - Maximum vane temperature as function of average vane temperature. (See table II for symbol definitions.)

Turbine inlet temperature potential. - Since the maximum vane temperature occurred generally at thermocouple position 4, the local temperature difference correlation (table III) was used to plot the allowable turbine inlet temperature as a function of the ratio of coolant flow to gas flow, as shown in figure 20. A maximum vane temperature of 1311 K (1900° F) and two coolant temperatures, 589 K (600° F) and 811 K (1000° F), are represented by the solid lines. This figure indicates that the vane investigated could operate at a turbine inlet temperature and pressure of 1922 K (3000° F) and 31 N/cm^2 (45 psia), a coolant temperature of 811 K (1000° F), and a coolant flow

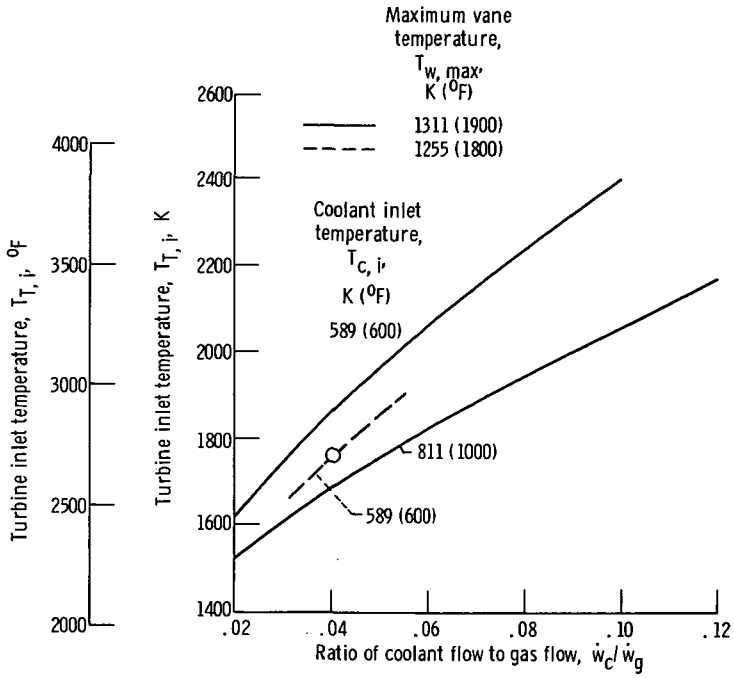

Figure 20. - Potential turbine inlet temperature as function of coolant flow and fixed maximum vane temperature and coolant inlet temperature.

ratio of 0.075. The dashed line represents the turbine inlet temperature to be expected for a coolant temperature of 589 K (600° F) and a maximum wall temperature of 1255 K (1800° F). A single experimental data point was taken at these approximate conditions with a coolant flow ratio of 0.04 and a turbine inlet temperature of approximately 1760 K (2710° F). The good comparison between the experimental data point (which was at a higher turbine inlet temperature than was used in the correlation) and the projected result shows that this method can be used to select higher turbine operating temperatures and the required coolant flow.

Airfoil temperature profiles. - A midspan vane temperature profile was calculated using the local φ curves discussed previously and the following assumptions: the max-

imum vane temperature was 1311 K (1900° F) and the coolant temperature was 811 K (1000° F) at coolant flows ratios of 0.04 and 0.08. The resulting turbine inlet temperatures should be 1683 K (2570° F) and 1939 K (3030° F), respectively. Figure 21 shows the calculated vane temperature profiles for a coolant flow ratio of 0.04 at the lower turbine inlet temperature (solid curve) and for a coolant flow ratio of 0.08 at the higher turbine inlet temperature (dashed curve). Comparison of the two curves shows that both conditions result in about the same maximum and average wall temperatures; however, the larger gradient associated with the higher turbine inlet temperature would result in a reduced life expectancy of the vane.

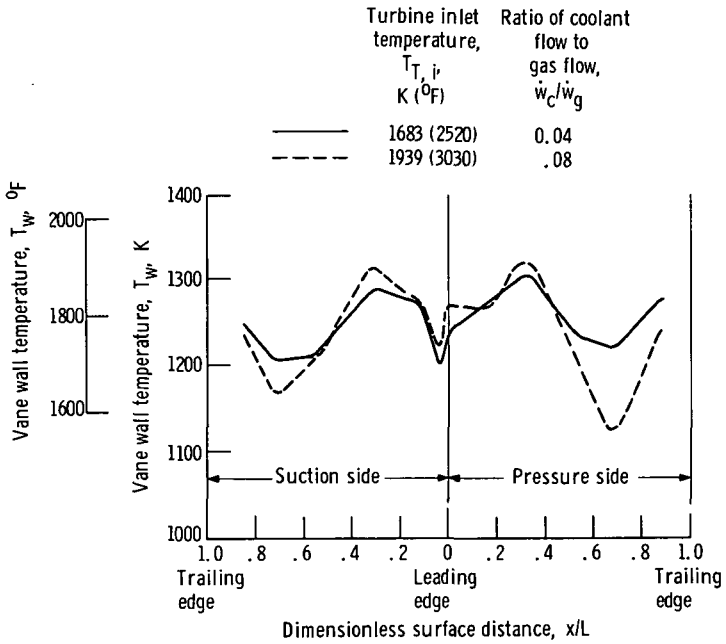

Figure 21. - Vane temperature profile calculated from φ_x, assuming a maximum wall temperature of 1311 K (1900° F) and a coolant inlet temperature of 811 K (1000° F).

General Comments

It was previously stated that the ideal way of estimating vane and blade wall temperatures would be to use purely analytical methods. Since such methods have not yet been perfected, recourse must be made to the use of empirical results. This report presents methods for correlation of cooled-turbine-vane heat-transfer data. If the correlations are to be used at higher heat flux (i.e., higher turbine inlet temperatures and/or pressures, where the temperature gradient through the vane wall becomes more significant),

further investigation is in order. Comments on each of these methods follow.

The first and theoretically the best correlation requires the determination of exponents for $(\dot{w}/\mu)_g$ and $(\dot{w}/\mu)_c$ from experimental data and the evaluation of gas and coolant property values. Lack of any measured coolant temperature other than the coolant inlet temperature and lack of information on local coolant flow rates had detrimental effects on this attempted correlation.

Another correlation was a simple plot of a measured temperature difference ratio against the ratio of coolant flow to gas flow. This correlation proved to be as good or better for the data presented herein than the other correlation, both for average and local vane midspan conditions. Its use is, therefore, recommended both because of the results presented and because of its ease in application. In fact, even for vane or blade designs for fixed conditions, this correlation can be used to estimate vane wall temperatures.

A value of $\varphi = 0.46$ was found for the vane operated at a turbine inlet temperature of 1644 K (2500° F), an inlet coolant temperature of 589 K (600° F), and a ratio of coolant flow to gas flow of 0.035. The average vane temperature was 1159 K (1626° F) and the thermal effectiveness η_t of the vane was calculated as 0.58. These results indicate the vane cooled satisfactorily.

SUMMARY OF RESULTS

The results of the experimental investigation report herein are summarized as follows:

1. Experimental heat-transfer data for an air-cooled turbine vane operated in a cascade at gas temperatures to 1644 K (2500° F) and pressures to 31 N/cm^2 (45 psi) were successfully correlated. Both average and local midspan vane temperatures were included.

2. The simplest correlation, temperature difference ratio φ as a function of the ratio of coolant flow rate to gas flow rate $\dot{w}_c/\dot{w}_g$, generally appeared best and is therefore recommended.

3. Measured midspan average temperatures differed by at most ±5 percent from those calculated using the $\overline{\varphi}$ correlation.

4. Measured and calculated coolant flow rates through sections of the vane agreed within about 10 percent.

5. Measured and predicted vane midspan temperature distributions agreed within ±15 percent or less.

6. For a maximum allowable vane temperature of 1311 K (1900° F), it was found from extrapolation of data that the vane could operate at a turbine inlet temperature of

1922 K (3000° F) with a coolant inlet temperature of 811 K (1000° F) and a ratio of coolant flow rate to gas flow rate of 0.075 at a pressure of 31 N/cm^2 (45 psia).

7. For a turbine inlet temperature of 1644 K (2500° F), a coolant inlet temperature of 589 K (600° F), and a ratio of coolant flow to gas flow of 0.035, the values of $\overline{\varphi}$ and η_t were found to be 0.46 and 0.58, respectively.

Lewis Research Center,
National Aeronautics and Space Administration,
Cleveland, Ohio, July 13, 1971,
764-74.

APPENDIX A

SYMBOLS

A	flow area
b	equivalent slot width
C_p	specific heat at constant pressure
c_m	mixing coefficient
c_n	center-to-center spacing
D	diameter
D_h	hydraulic diameter
d	pin fin diameter
E	coefficient (table III)
F	exponent (table III)
g	acceleration due to gravity
h	heat-transfer coefficient
J	mechanical equivalent of heat
K, K_1, K_2, K_3	constants
k	thermal conductivity
L	length of vane surface
M	$\rho v_c/\rho v_g$
m, n	exponents
Nu	Nusselt number
P	pressure
Pr	Prandtl number
Re	Reynolds number
r	radius
S	heat-transfer area
s	slot width
T	temperature
v	velocity
W	relative velocity
$\dot{w}$	flow rate
x	distance along surface from stagnation point or distance from film-cooling slot
Y	defined by eq. (B11)
z_n	distance from nozzle to impingement surface
η_f	$(T_{ge} - T_{aw})/(T_{ge} - T_{c,s})$
η_t	$(T_{c,o} - T_{c,i})/(T_w - T_{c,i})$
θ	angle measured from stagnation point
Λ	recovery factor
λ	$h_g S_g/h_c S_c$
μ	viscosity
ρ	density
φ	$(T_{ge} - T_w)/(T_{ge} - T_e)$

Subscripts:

a	arrival
aw	adiabatic wall
c	coolant
conv	convection
corr	corrected
f	film
g	gas

ge	effective gas
i	inlet
le	leading edge
le,x	leading-edge exit
m	measured
max	maximum
mc	midchord
n	nozzle
o	exit
P	pressure surface
ref	reference
S	suction surface
s	slot
st	static
te	trailing edge
T,i	turbine inlet
tot	total
w	wall
x	local
y	spanwise distance

Superscripts:

''	relative total
-	average

APPENDIX B

CORRELATION OF METAL TEMPERATURES

Consider a one-dimensional heat balance across a segment of a convection and film-cooled wall. Assuming that the wall temperature is constant, the heat-balance may be written as

$$h_g S_g (T_{aw} - T_w) = h_c S_c (T_w - T_c) \tag{B1}$$

or by rearranging equation (B1), as

$$\varphi = \frac{1 + \lambda \eta_f \left(\frac{T_{ge} - T_{c,s}}{T_{ge} - T_c} \right)}{1 + \lambda} \tag{B2}$$

where

$$\varphi = \frac{T_{ge} - T_w}{T_{ge} - T_c} \tag{B3}$$

$$\lambda = \frac{h_g S_g}{h_c S_c} \tag{B4}$$

and

$$\eta_f = \frac{T_{ge} - T_{aw}}{T_{ge} - T_{c,s}} \tag{B5}$$

For the case of convection cooling only (i.e., $\eta_f = 0$), φ reduces to the form of reference 1, that is,

$$\varphi = \frac{1}{1 + \lambda} \tag{B6}$$

Equation (B2) can be rearranged and written as

$$\frac{1 - \varphi}{\varphi} = \lambda \left[1 - \frac{\eta_f}{\varphi} \left(\frac{T_{ge} - T_{c,s}}{T_{ge} - T_c} \right) \right] \tag{B7}$$

Expressing the gas-to-wall and wall-to-coolant heat-transfer coefficients as

$$h_g = K_1 \frac{k_g}{L} Re_g^n Pr_g^{1/3} \tag{B8}$$

$$h_c = K_2 \frac{k_c}{D_h} Re_c^m Pr_c^{1/3} \tag{B9}$$

introducing the definitions of Re_g and Re_c and rearranging, equation (B7) may be written as

$$\frac{Y}{\left(\frac{\dot{w}}{\mu}\right)_g^n \left(\frac{\mu}{\dot{w}}\right)_c^m} = K \left[1 - \frac{\eta_f}{\varphi} \left(\frac{T_{ge} - T_{c,s}}{T_{ge} - T_c} \right) \right] \tag{B10}$$

where

$$Y = \frac{1 - \varphi}{\varphi} \frac{Pr_c^{1/3} k_c}{Pr_g^{1/3} k_g} \tag{B11}$$

and K is a constant. For the case of no film cooling, $\eta_f = 0$ and equation (B10) reduces to

$$Y = K \left(\frac{\dot{w}}{\mu}\right)_g^n \left(\frac{\mu}{\dot{w}}\right)_c^m \tag{B12}$$

REFERENCES

1. Livingood, John N. B.; and Brown, W. Byron: Analysis of Spanwise Temperature Distribution in Three Types of Air-Cooled Turbine Blade. NACA Rep. 994, 1950.

2. Stepka, Francis S.; and Richards, Hadley T.: Experimental Investigation of Metal Temperatures of Air-Cooled Airfoil Leading Edges at Subsonic Flow and Gas Temperatures up to 2780° F. NASA TN D-127, 1959.

3. Stepka, Francis S.: Considerations of Turbine Cooling Systems for Mach 3 Flight. NASA TN D-4491, 1968.

4. Clark, John S.; Richards, Hadley T.; Poferl, David J.; and Livingood, John N. B.: Coolant Pressure and Flow Distribution Through an Air-Cooled Vane for a High-Temperature Gas Turbine. NASA TM X-2028, 1970.

5. Calvert, Howard F.; Cochran, Reeves P.; Dengler, Robert P.; Hickel, Robert O.; and Norris, James W.: Turbine Cooling Research Facility. NASA TM X-1927, 1970.

6. Crowl, Robert J.; and Gladden, Herbert J.: Methods and Procedures for Evaluating, Forming, and Installing Small-Diameter Sheathed Thermocouple Wire and Sheathed NASA TM X-2377, 1971.

7. Katsanis, Theodore; and Dellner, Lois T.: A Quasi-Three-Dimensional Method for Calculating Blade Surface Velocities for an Axial Flow Turbine Blade. NASA TM X-1394, 1967.

8. Katsanis, Theodore: FORTRAN Program for Calculating Transonic Velocities on a Blade-to-Blade Stream Surface on a Turbomachine. NASA TN D-5427, 1969.

9. Gladden, Herbert J.; Dengler, Robert P.; Evans, David G.; and Hippensteele, Steven A.: Aerodynamic Investigation of Four-Vane Cascade Designed for Turbine Cooling Studies. NASA TM X-1954, 1970.

10. Kreith, Frank: Principles of Heat Transfer. International Textbook Co., 1958.

11. Rohsenow, Warren M.; and Choi, Harry Y.: Heat, Mass, and Momentum Transfer. Prentice-Hall, Inc., 1961.

12. Eckert, Ernst R. G.; and Drake, Robert M., Jr.: Heat and Mass Transfer. Second ed., McGraw-Hill Book Co., Inc., 1959.

13. Juhasz, A. J.; and Marek, C. J.: Combustor Liner Film Cooling in the Presence of High Free-Stream Turbulence. NASA TN D-6360, 1971.

14. Schlichting, Hermann (J. Kestin, Trans.): Boundary Layer Theory. Fourth ed., McGraw-Hill Book Co., Inc., 1960, p. 401.

15. Hickel, Robert O.; and Smith, Gordon T.: Experimental Investigation of Air-Cooled Turbine Blades in Turbojet Engines. III - Rotor Blades with 34 Steel Tubes in Cooling-Air Passages. NACA RM E50J06, 1950.

16. Gladden, Herbert J.; Hippensteele, Steven A.; Hickel, Robert O.; and Dengler, Robert P.: Radiation Heat-Transfer Characteristics of Turbine Vane Airfoils in a Water-Cooled Cascade. NASA TM X-2203, 1971.

17. Chupp, R. E.; Helms, H. E.; McFadden, P. W.; and Brown, T. R.: Evaluation of Internal Heat Transfer Coefficients for Impingement Cooled Turbine Airfoils. Paper 68-564, AIAA, June 1968.

18. Gardon, Robert; and Cobonpue, John: Heat Transfer Between a Flat Plate and Jets of Air Impinging on It. International Developments in Heat Transfer. ASME, 1963, pp. 454-460.

19. Theoclitus, G.: Heat-Transfer and Flow Friction Characteristics of Nine Pin-Fin Surfaces. J. Heat Transfer, vol. 88, no. 4, Nov. 1966, pp. 383-390.

20. Poferl, David J.; Svehla, Robert A.; and Lewandowski, Kenneth: Thermodynamic and Transport Properties of Air and the Combustion Products of Natural Gas and of ASTM-A1 Fuel with Air. NASA TN D-5452, 1969.

NASA-Langley, 1971 — 33 E-6230

"The aeronautical and space activities of the United States shall be conducted so as to contribute . . . to the expansion of human knowledge of phenomena in the atmosphere and space. The Administration shall provide for the widest practicable and appropriate dissemination of information concerning its activities and the results thereof."

— NATIONAL AERONAUTICS AND SPACE ACT OF 1958

NASA SCIENTIFIC AND TECHNICAL PUBLICATIONS

TECHNICAL REPORTS: Scientific and technical information considered important, complete, and a lasting contribution to existing knowledge.

TECHNICAL NOTES: Information less broad in scope but nevertheless of importance as a contribution to existing knowledge.

TECHNICAL MEMORANDUMS: Information receiving limited distribution because of preliminary data, security classification, or other reasons.

CONTRACTOR REPORTS: Scientific and technical information generated under a NASA contract or grant and considered an important contribution to existing knowledge.

TECHNICAL TRANSLATIONS: Information published in a foreign language considered to merit NASA distribution in English.

SPECIAL PUBLICATIONS: Information derived from or of value to NASA activities. Publications include conference proceedings, monographs, data compilations, handbooks, sourcebooks, and special bibliographies.

TECHNOLOGY UTILIZATION PUBLICATIONS: Information on technology used by NASA that may be of particular interest in commercial and other non-aerospace applications. Publications include Tech Briefs, Technology Utilization Reports and Technology Surveys.

Details on the availability of these publications may be obtained from:

SCIENTIFIC AND TECHNICAL INFORMATION OFFICE

NATIONAL AERONAUTICS AND SPACE ADMINISTRATION

Washington, D.C. 20546